ansto

Replacement Research Reactor Project

SUBMISSION TO ARPANSA ON THE SITE GEOLOGICAL INVESTIGATIONS FOR THE REPLACEMENT RESEARCH REACTOR AT LUCAS HEIGHTS

Prepared By
the
Australian Nuclear Science and Technology Organisation

12 SEPTEMBER 2002

ANSTO		Document No.: **RRRP-7500-3BEAN-002-A** Revision: **A**			
Replacement Reactor Project		Document Title: **SUBMISSION TO ARPANSA ON THE SITE GEOLOGICAL INVESTIGATIONS FOR THE REPLACEMENT RESEARCH REACTOR AT LUCAS HEIGHTS**			
REVISION SHEET		Ref. No.:			
		Indicate name, date and signature or initial			
Revision Letter	Description of Revision	Prepared	Checked/ Reviewed	Approved	Agreed
A		RFC	RM	GDW	

Notes: 1. The revision must be verified in accordance with the Quality Plan for the job.
2. Revision to be agreed by the Client where relevant.

EXECUTIVE SUMMARY

BACKGROUND

As a result of a recommendation from the IAEA Peer Review of the PSAR in June 2001, ANSTO agreed to undertake a detailed seismic assessment of the site and nearby area to supplement the information made available in the PSAR. The nearby site study was completed in January 2002 and submitted to ARPANSA. This report describes the outcomes of the studies that were done on the excavations at the site, following the issue of the Facility Licence, Construction Authorisation in April 2002. Since no guidelines exist for reporting on these issues for research reactors, ANSTO has conservatively followed the guidelines issued by the International Atomic Energy Agency for nuclear power plants.

Many previous assessments exist of the geology and seismology of the Lucas Heights region. These have been reported in the Environmental Impact Statement and in the Preliminary Safety Analysis Report. They include a range of geophysical, geotechnical and seismological analyses performed independently by experts in these fields. The Replacement Research Reactor (RRR) has been designed in the light of these studies and with a design seismic hazard spectrum that bounds all previous recommendations.

REGIONAL GEOLOGY

Sydney is located towards the centre of the Sydney Basin. The basin extends northwards from Bateman's Bay to approximately 200 km north-northwest of Botany Bay. The basin contains Early Permian to Middle Triassic sedimentary marine and terrestrial strata and volcanic rocks. At the western margin of the Sydney Basin, basin fill comprising Permian coal measures laps onto, and unconformably overlies, Lachlan Fold Belt rocks. The northeast margin of the Sydney Basin is defined by the faulted contact of Sydney Basin rocks against Paleozoic rocks of the New England Fold Belt along the Hunter-Mooki thrust fault.

Sydney Basin sedimentary rocks consist of non-marine coal measures grading up into Triassic and possibly early Jurassic terrestrial and estuarine sandstone and siltstone. Most faulting activity in the Sydney Basin occurred as a result of the Tasman Sea opening 83-53 million years ago.

Typical fault displacements are less than 15 m but occasional displacements of up to 100 m and bed dips of $< 5°$ have been reported. The Lapstone Structural Complex is a prominent tectonic and physiographic feature of the Sydney Basin. It consists of a number of related folds and faults, tending generally north-south, coincident with the eastern margin of the Blue Mountains. It is located about 60km west of Sydney and 35km west of Lucas Heights. The complex is more than 100km long and generally about 2 to 5km wide.

Detailed analysis of faults from the Southern Coalfield (south of the RRR site) and from tunnels excavated within Hawkesbury Sandstone (north of the RRR site) indicate predominantly net normal fault displacements on two main sets which strike approximately northwest and north to north-northeast. Analysis of these data confirm that:

- There is extensive data on the geology and seismology of the Sydney Basin.
- Widespread faulting has been observed throughout the region and mapped extensively in the

coal mines and as part of tunnel data for new roads and water/sewage transport channels.

- The two main fault directions in the region are northwest and north-northeast. In displacement terms, the northwest striking faults are the dominant set. The fault strands on the RRR site belong to the north-northeast set.
- Normal faults have been seen, on average, every 140 metres in the tunnel data and apparently reverse faults every 1-3 km. These sets of faults have generally small displacements (less than 15 metres).
- The geology and fault characteristics of the RRR site are consistent with the general pattern of extensive faulting that persists in the local region, a region of low tectonic activity.

NEAR FIELD STUDY

The near field study, reported in January 2002, presented the results of a desk study and field reconnaissance of an area within 5 km of the RRR site. Fault and lineament data, compiled from rock exposures (i.e. road cuttings, natural exposures along tributaries of the Woronora River, and quarry walls) were examined in an area up to 5 km from the RRR site. Existing data were compiled from published reports. Fieldwork was carried out following completion of the desk study that included an aerial photographic interpretation of available colour aerial photographs. The study concluded that field reconnaissance of accessible soil and rock exposures within 5 km of the RRR site, revealed only a few small-scale normal faults with displacements less than 0.3m. None of these faults displaces soils and near-surface material. There is no evidence that these faults are active and pose an earthquake hazard for the RRR site.

MAPPING OF THE SITE AND EXCAVATIONS

The second part of the seismic assessment was designed to document fractures (i.e. faults and joints) in rocks exposed in road batters and in the foundation excavation of the Reactor and Neutron Guide Halls at the RRR site. Fieldwork for this part of the investigation, referred to as Task 2 was completed between April and June, 2002.

This detailed geological mapping of the RRR site led to the identification, measurement and analysis of two main fault strands in bedrock exposures on the RRR site. These generally strike to the north-northeast (000-020°), dip steeply (mostly 65-80° east and west) and have dip separations of c. 1-1.3 m (the eastern strand) and c. 0.20-0.32 m (the western strand), which are seen in the reactor excavations. Some smaller faults are clustered around these dominant structures.

In net displacement terms, the eastern fault strand is an apparent normal fault and is the dominant fault trace observed at the RRR site. The fault extends for at least 140 m across the site in a north-northeast direction (mean strike 013°) and dips steeply to the east (mean dip 67°). Within the area comprising the footprint for the Reactor Building, the fault has a constant dip separation of c. 1-1.3 m up through the rock sequence and across the excavation. The western fault strand is the second largest faulting trace observed at the RRR site and has apparent displacement in an opposite direction to the normal fault. This fault trace extends for at least 120 m across the site in a north-northeast direction (mean strike 009°) and dips steeply to the east. The two main fault strands converge in the northern part of the site to form a single fault zone.

ADDITIONAL INVESTIGATIONS AND DATING

Following discovery of the faulting, additional investigations were undertaken to determine their relevance for the construction of the RRR. Several consultants examined the information and two alternative interpretations have been proposed.

1. In the first interpretation both the eastern and western strands were formed during the opening of the Tasman Sea i.e. 53-83 million years ago, and inhomogeneity in the strata or the stress field influenced the nature of the movement on the western strand. This hypothesis is supported by two main arguments. First, the fault plane dips at a somewhat steeper angle than would be expected for a true reverse fault. Second, and more important, the exposure of the same fault on the north face of the main excavation is normal in character and downthrown to the west. Further a series of small dykes up to approximately 0.5 m wide occurs to the west of the main excavation, which predates any potential fault movement. The dykes occupy a set of fractures that have a similar orientation to the normal faults and do not appear to have seen any significant disruption.

2. In the second interpretation, the eastern and western strands are part of a system that initiated as a normal fault system, formed during the Tasman Sea opening 83-53 million years ago, with reverse reactivation occurring on one of the strands, and possibly both. This is the most conservative explanation because the reactivation is inferred to have occurred more recently than the Tasman Sea opening.

The first interpretation would immediately render the faulting as not capable, because any movement would have occurred between 83 and 53 million years ago. Such faulting is typical of the vast majority of the faults in the Hawkesbury Sandstone, particularly within approximately 10 km of the coast.

The second interpretation suggests that the reactivation occurred sometime after 83-53 million years ago. Hence further analysis performed for this report was performed to test this conservative assumption and to date movements on the western strand using both numerical and relative modern dating methods.

Three approaches were used to constrain the age of the faulting in the foundation excavation for the RRR. One was to find and date material from the region of the fault itself. The second was to analyse borehole material to date a pervasive deep weathering episode that followed fault movement. The third was to trace the fault to an area where there was overlying material that could be studied, both in terms of geomorphology and for dating purposes. An assessment of the age of nearby related dykes was also made. A number of trenches were dug to trace the fault across the site and a trench was dug to the north of the site, where the fault was evident in the bedrock and where the younger overlying material was clearly not affected by the fault.

A wide range of possible dating methods was considered. The choice depends on the types of material that are available either in the fault itself or in the cover material above the fault. For this study, both direct numerical dating and relative dating methods were used. These included:

- Study of the geomorphology and geochronology of the material in a trench where cover existed above the fault.

- Optically Stimulated Luminescence (OSL) to date the unfaulted strata that overlie the fault in the trench.
- Paleomagnetic dating using the magnetic signature of the rocks and relating that to the information known on magnetic reversals and on movements of the earth's magnetic pole. This was done both for material crossing the fault and with samples taken at various locations in trenches.
- Fission track and (U-Th)/He dating of borehole material. The results constrain the total depth and timing of deep erosion which has occurred over the area and provide another minimum age estimate for the time of faulting.

The results obtained provide a consistent picture of the age of the material in the fault and overlying the fault. The Optically Stimulated Luminescence data give consistent ages of the overlying Quaternary material that range from 14,000 years in the upper aeolian layers to greater than 104,000 years in the sand layers above the fault itself. There was no evidence that these layers have been displaced by the fault. Given the fact that this material appears to have been transported to the site and may have been subject to various removal and replacement cycles, these ages are much younger than the fault itself. Both the paleomagnetic analysis of the clasts at the bedrock to cover interface and the geomorphology confirm that the material has been transported to the site and probably replaced several times since the fault developed, and is not simply weathered bedrock.

On the basis of the thermochronology, a consistent picture emerges of the major episodes of movement and deposition. The age of the deep weathering episode, which post-dated the fault movement, provides an unambiguous constraint on the last possible time of fault movement and gives an interval of 35-10 million years since the last movement.

Paleomagnetic results of ferruginous material laid down across the fault and post dating any movement along the fault provide a direct assessment of the limiting age of the most recent movement of the fault. Analysis of the iron oxides in this material yields a mean age of 9 million years and not younger than 5 million years. That is, using the most conservative interpretation, there has been no fault movement for at least 5 million years.

COMPARISON WITH INTERNATIONAL CRITERIA

The key issue for assessment of the fault is whether the fault is deemed to be 'capable' i.e. whether the fault has significant potential for relative displacement at or near the ground surface. The two main sets of criteria for Power Reactors, there being no specific criteria for the much smaller research reactors, are those from the US Nuclear Regulatory Commission (NRC) and the International Atomic Energy Agency (IAEA). The findings of the investigations have been compared with both criteria but here we present the comparison with the more rigorous criteria from the IAEA to assess the capability of the faulting seen in the RRR site.

The IAEA Safety Guide (50 SG-S1, 1991) sets out criteria for determining capability. The basis for answering such a question should be the database of geological and seismological investigations. Using the IAEA definition, a fault shall be considered capable if:

1. *It shows evidence of past movement or movements of a recurring nature within such a period that it is reasonable to infer that further movement at or near the surface can occur. (In*

highly active areas, where both earthquake and geological data consistently reveal short earthquake recurrence intervals, periods of the order of tens of thousands of years may be appropriate for the assessment of capable faults. In less active areas, it is likely that much longer periods may be required.)

As discussed in this report, the most recent fault movement is at least 5 million years old, the thermochronology indicates a minimum of 10 million years, and the fault shows no evidence of past movement or movements of a recurring nature within such a period that it is reasonable to infer that further movement at or near the surface can occur.

2. *A structural relationship has been demonstrated to a known capable fault such that movement of the one may cause movement of the other at or near the surface.*

The nearest known possible Capable Fault to the site fault is the Lapstone Structural Complex located approximately 35 km west of the site. Because of this substantial distance no secondary movement is expected to occur on the site fault. In addition, a considerable amount of geological and geophysical investigation has taken place between the Lapstone Structural Complex and the coast, related to coal and gas exploration. These investigations have proved conclusively that similar zones to the Lapstone Structural Complex do not extend further east towards Lucas Heights. Structural geology considerations also place the Lapstone Structural Complex in a separate tectonic zone, west of the coastal zone in which the site occurs.

3. *The maximum potential earthquake associated with a seismogenic structure, as determined in section 4, is sufficiently large and at such a depth that it is reasonable to infer that movement at or near the surface can occur.*

The only seismogenic structure is the Lapstone Structural Complex. The conservative choice for the repeat time for the Lapstone Structural Complex is 11-27 ka, so the Lapstone Structural Complex will have ruptured many times during the past 5-13 million years and clearly has not triggered any slip at the RRR site. That covers triggered slip. At a more elementary level one may also ask about direct co-seismic slip. For this to happen, the RRR site fault would need to be part of the same structure as the Lapstone Structural Complex and clearly it is not.

Therefore, the site fault cannot be classified as Capable by the criteria established by the IAEA for the siting of nuclear power plants.

CONCLUSIONS

The faults discovered in the reactor excavations have been extensively studied and the minumum age of the last movement has been determined by the paleomagnetism results as 5-13 million years ago, consistent with the thermochronology results of 10-35 million years. Therefore these faults are clearly not potential seismic sources, even under the most conservative assumption on the age of last movement of the fault discovered in the RRR excavation, and they do not pose a surface-fault rupture hazard. This confirms that there is no need to alter the outcomes of the analysis already performed as part of the probabilistic seismic hazard assessment and used in the design of the reactor. This analysis considered the appropriate peak ground acceleration and hazard spectrum to be used for the Lucas Heights region, based on the overall seismicity of the region. Given this conclusion, and the conservative nature of the design process, there is no change required to the design hazard spectrum or the facility design, put forward in the PSAR in May 2001.

TABLE OF CONTENTS

PURPOSE AND SCOPE OF THE SUBMISSION

1.1 PURPOSE

As a result of a recommendation from the IAEA Peer Review of the PSAR in June 2001, ANSTO agreed to undertake a detailed seismic assessment of the site and nearby area to supplement the information made available in the PSAR. The nearby site study was completed in January 2002 and submitted to ARPANSA. This report describes the outcomes of the studies that were done on the excavation of the site, following the issue of the Facility Licence, Construction Authorisation in April 2002.

1.2 SCOPE

This report describes the regional and near site studies (as background), the geological mapping of the site, the assessment of the fault type and characteristics found in the excavated area, the assessment made of the similarity of the fault to the information known about faults in the region, the dating of the fault and the comparison with criteria on fault capability.

2 BACKGROUND

Following an Environmental Impact Statement, lodged in August 1998 and finalised in January 1999, and the issue of a site licence by ARPANSA in September 1999, ANSTO commenced the detailed design and preparation of the safety analysis. This was submitted to ARPANSA in May 2001 and a construction licence was granted in April 2002.

As part of the safety analysis and verification of the site, and in response to an IAEA recommendation accepted by ARPANSA, ANSTO commissioned the New Zealand Institute of Geological and Nuclear Sciences (GNS) and Coffey Partners to undertake a near site investigation (out to 5 km) and an assessment of the excavated site. The near field investigation was reported in January 2002 and revealed no evidence of active faults. During the assessment of the excavations, which could only follow the issue of the construction licence in April 2002, faulting was discovered. Work stopped in June 2002 to allow investigation of the significance of these faults.

There are no universally accepted methodologies for performing geological and seismological site assessments for a research reactor. Guidelines do exist for nuclear power plants (IAEA, 1991) but such reactors have a much higher radioactive inventory and more severe operating conditions (of temperature and pressure) than research reactors. Hence the hazard they pose is much greater. In the absence of specific requirements for research reactors, ANSTO has used the regulatory guidelines for nuclear power plants, which are conservative for this type of facility. In following this approach, ANSTO has conducted geological and seismological investigations of the site for the Replacement Research Reactor (RRR) which are fully consistent with the guidelines provided by the IAEA for power reactors. Table 2.1 shows the comparison with the IAEA guidelines on geological information.

Table 2.1 Comparison of geological assessments with IAEA guidelines

IAEA Guideline Section 3 of SS 50 SG S1 (1991)	Section of this report
Regional study containing all the information that potentially affects the seismic hazard at the site (typically out to 150 km).	Alliance report (1999), Chapter 3 of the PSAR and Section 3 of this report
Near regional study to define the seismotectonic characteristics of the near region (out to 25 km).	Regional study as presented in Section 4 of this report
Site vicinity study out to 5 km to understand the potential for permanent ground deformation, including surface faulting.	Near site study, presented in Section 5
Site area study, up to 1 km^2 to add detailed knowledge on the potential for permanent displacement.	See section on mapping of the site and the excavations in Section 6.

3 PREVIOUS ASSESSMENTS OF THE GEOLOGY, GEOPHYSICS AND SEISMOLOGY OF THE LUCAS HEIGHTS REGION

Previous assessments have provided significant information on the geology and seismology of the region surrounding the Lucas Heights Science and Technology Centre (LHSTC).

A generalised descriptive understanding of the LHSTC geology was available from literature sources (e.g. Sherwin & Holmes, 1986) prior to site specific Replacement Research Reactor (RRR) investigations commencing with the Environmental Impact Statement (EIS).

A geophysical study of the RRR site was conducted by Coffey Partners International as part of the EIS (Coffey 1998a) including seismic refraction, resistivity soundings and magnetometer surveys. The magnetometer survey identified anomalies to the north of the RRR site considered to be an extension of a minor dyke structure seen near the Little Forest Burial Ground. The strike of the dyke is north-northeast and projects to the west of the RRR site. Minor magnetic anomalies were also detected which may have indicated a feature projecting onto the RRR site. Follow-up with a detailed magnetic survey of the RRR site failed to detect any evidence for the presence of a dyke.

A geohydrological and hydrochemical study of the RRR site was conducted by Coffey Partners International as part of the EIS (Coffey 1998b) for the purpose of better understanding the groundwater of the RRR site.

Two geotechnical studies of the RRR site were conducted by Coffey Partners International as part of the provision of design data specific to the site (Coffey 1998c and Coffey 1999) including borehole logging, examination of shallow pits, seismic tomographic imaging and downhole acoustic logging. These studies did not indicate any significant geological structures such as faults, dykes, etc. within the site.

A near-site investigation was undertaken for ANSTO by Coffey Geosciences Pty Ltd, formerly Coffey Partners, (Coffey 1999b) to determine whether there is any evidence of small-scale surface faulting of the form identified in some parts of the Sydney area and to further assess the nature of the lower velocity zone located near the western site boundary that was previously identified (Coffey 1998a). The investigation involved review of previous site investigation reports, aerial photographic interpretation and reconnaissance-level geological mapping. This study identified only minor geological features.

A seismic hazard analysis of the Lucas Heights site was undertaken for the Department of Industry, Science, and Resources by a project team from the GNS (Wellington), Seismological Research Centre (Melbourne), Dames & Moore Ltd. (San Francisco and Seattle), and William Lettis & Associates (San Francisco). This analysis included a review of the earthquake ground shaking hazard at Lucas Heights using best international practice as determined from a review of current US and international procedures (Alliance, 1999).

The study utilised the most complete computer catalogue of New South Wales earthquakes; that is maintained by the Australian Seismological Centre. That catalogue was modified and extended for this study, particularly for earthquakes before 1900. The seismic source model used in this study was based on regional geology then modified considering distribution and rate of historical seismicity. Source zones corresponding to the Sydney Basin, the Lachlan Fold Belt and the New England Fold Belt were defined. These were then divided into five zones based on seismicity (Figure 3.1). The outcomes from the study were predicted mean peak ground accelerations and response spectral accelerations for a range of return periods.

An extension to that seismic hazard analysis was undertaken for ARPANSA by GNS to address issues raised in local and international reviews of the Alliance (1999). The report on this additional work (Stirling & Berryman, 2001) provided modified predicted mean peak ground accelerations and response spectral accelerations for a range of return periods.

Using conservative analysis techniques, the RRR has been designed to, as a minimum, withstand the predicted mean peak ground accelerations and response spectral accelerations for an earthquake return period of 10,000 years.

4 REGIONAL GEOLOGY OF THE SYDNEY BASIN

The geology of the Sydney Basin is discussed below to provide the geological context for the near site study and site investigations that were commissioned by ANSTO and undertaken by GNS. Figure 4.1 shows a map of the Sydney Basin, showing the main locations of interest.

4.1 ROCK UNITS

Sydney is located towards the centre of the Sydney Basin. The basin extends northwards from Bateman's Bay to approximately 200 km north-northwest of Botany Bay. The basin contains Early Permian to Middle Triassic sedimentary marine and terrestrial strata and volcanic rocks (see Herbert & Helby, 1980). At the western margin of the Sydney Basin, basin fill comprising

Permian coal measures laps onto, and unconformably overlies, Lachlan Fold Belt rocks. The northeast margin of the Sydney Basin is defined by the faulted contact of Sydney Basin rocks against Paleozoic rocks of the New England Fold Belt along the Hunter-Mooki thrust fault.

Table 4.1 shows the main periods and their associated features.

Period	**Feature**
Pre Permian (>300 Ma∗)	The Lachlan Fold Belt (which outcrops to the west and underlies much of the Sydney Basin) has a strong north-south tectonic trend.
Permian (300-250 Ma)	Sedimentation commenced in the Sydney Basin, with some structural deformation during sedimentation.
Triassic (250-205 Ma)	• Deposition of Narrabeen Group and Hawkesbury Sandstone Formation. • Structural control on thickness and nature of sediments deposited, due to basement deformation and contemporaneous tectonism.
Late Cretaceous-Early Tertiary (83-53 Ma)	• Tasman Sea opens • Variable periods/regions of tension and compression. • Episodic faulting, including strike-slip movements • Blue Mountains uplifted.
Eocene (55-38 Ma)	• Period of tension and dyke intrusion.
Post Eocene (38-0 Ma)	• Localised volcanism to about 26 Ma • Some movement of Lapstone-Kurrajong structures • East-west compression is main horizontal stress direction.

∗ Ma = million years

Sydney Basin sedimentary rocks consist of non-marine coal measures grading up into Triassic and possibly early Jurassic terrestrial and estuarine sandstone and siltstone (Herbert, 1980). The absence of younger Mesozoic rocks is attributed by Ollier (1982) and Jones & Clark (1991) to erosion induced by uplift and doming as a precursor to the opening of the Tasman Sea about 83 to 53 million years ago (Sdrolias et al., 2001). Thin Tertiary-age rocks occur within the Sydney Basin, most notably in the Penrith Basin adjacent to the Lapstone Structural Complex (LSC) (Mauger et al., 1984) where several tens of metres of conglomerate, sand and clay represent ancient fluvial terrace and overbank flood deposits. Fan deposits are also locally significant along the LSC. In the coastal area, a significant thickness of estuarine and shallow marine deposits accumulated on the continental shelf during fluctuating Quaternary sea levels during the last c. 1.6 million years. At the coast, the height of Last Interglacial (c.125,000 years ago) marine deposits are about the same elevation above present sea level as at their time of formation, indicating vertical tectonic stability in coastal areas (Murray-Wallace & Belperio, 1991).

Basin rocks thin to the west from a maximum known thickness of 5000 to 6000 m at the edge of the continental shelf (Mayne et al., 1974). In the metropolitan Sydney region basin fill is typically 2200-3000 m thick. Data from a borehole sunk in 1965 near the main gate of the ANSTO facility at Lucas Heights indicates that the RRR site is underlain by 194 m of the Middle Triassic (c. 225 million years in age) Hawkesbury Sandstone formation, which overlies a further 458 m of interbedded sandstones and claystones of the Triassic Narrabeen Group. These Triassic sedimentary strata are in turn underlain by at least 884 m of Permian rocks. Data from the 1:100,000 Wollongong-Port Hacking Geological Sheet (Sherwin & Holmes, 1986) indicate that Permian rocks, which consist of coal, clastic and volcanic units, are approximately 1200-1500 m thick beneath the RRR site.

The main rock unit cropping out in the region of Lucas Heights is the Hawkesbury Sandstone formation (Sherwin & Holmes, 1986). The Hawkesbury Sandstone typically consists of medium to coarse-grained quartzose sandstone, with minor shale and laminated fine sandstone and mudstone beds. Sandstone beds are well indurated and commonly cross-bedded or horizontally bedded. This formation is interpreted to have been deposited in an extensive braided fluvial system (e.g., Herbert, 1980).

4.2 IGNEOUS DYKES

Igneous intrusive rocks are widespread in the greater Sydney region (Rickwood, 1985). Within the Sydney Basin basic dykes are common and typically strike northwest-southeast. The dykes are commonly steeply dipping, range in thickness from a centimetre to six metres and are usually deeply weathered near the surface. The dykes recognised on the RRR site typically trend to the north-northeast. Dykes were intruded into Sydney Basin strata during two main periods at 207-163 and 58-26 million years before present (e.g., Rickwood, 1985) but some are as young as 18.8 million years.

4.3 GEOLOGICAL STRUCTURES

Rocks of the Sydney Basin have been weakly deformed by a series of tectonic events. Typical fault displacements are less than 15 m but occasional displacements of up to 100 m and bed dips of < 5° have been reported. On a regional scale this deformation is manifest as a number of plateaux separated by monoclines (Bembrick et al., 1980).

The Lapstone Structural Complex is a prominent tectonic and physiographic feature of the Sydney Basin. It consists of a number of related folds and faults, tending generally north-south, coincident with the eastern margin of the Blue Mountains. It is located about 60km west of Sydney and 35km west of Lucas Heights. The complex is more than 100km long and generally about 2 to 5km wide. The complex incorporates a number of named structures, including the Nepean, Glenbrook, Kurrajong and Burralow faults. It is apparent that the Lapstone Structural Complex has had a long history with early deformation clearly influencing sedimentation within the Sydney Basin. It forms a boundary between two regions that have been subjected to a much lower level of tectonic activity.

The complex has been examined in some detail both by mapping and by seismic reflection surveys. Deformation has been by both folding and faulting, but different investigations have placed a range of interpretations on the relative contributions of folding and faulting (Herbert, 1988; Branagan 1969; Branagan & Pedram, 1990). It is often difficult to determine the throw of faults due to the absence of key horizons in the Hawkesbury Sandstone.

Analysis of seismic survey results over a 55km long segment of the complex north of Picton by Herbert (1988) indicates a maximum displacement of 100 metres in any individual fault plane, with displacements being generally less than 60 metres. Where the complex has been mapped in detail, these faults (and others located in the lower Blue Mountains such as the Oakdale Fault) appear to consist of relatively short parallel and sub-parallel segments. Displacement along each fault decreases rapidly towards each extremity.

There is a general consensus concerning the timing of major structural events in the Sydney Basin, although there is a degree of ongoing debate about the relative importance of these events in determining the current structure and ongoing tectonic activity. The main item of debate is whether the Triassic (250-205 million years) or Late Cretaceous (80-60 million years) periods of tectonic activity had the most impact. The consensus is that the earlier (Triassic) structures were the loci for later, larger deformations, which took place at the end of the Cretaceous with the opening of the Tasman Sea. Since that time, variable periods of extension and compression have been reflected in warping and episodic fault reactivation. Changes in the relative behaviour of the underlying basement and the Sydney Basin rocks to east-west compression have caused episodic fault reactivation. Offset by the Kurrajong fault of an early Miocene basalt dated at 18.8 million years (Wellman & McDougall, 1974) may indicate no more than a few tens of metres of displacement in this time. No Quaternary age fault scarps have been identified along the structure.

There has been a considerable amount of geological and geophysical investigation in the area between the Lapstone Structural Complex and the coast, related to coal and gas exploration. These investigations have found no evidence of similar zones to the Lapstone complex to the east towards Lucas Heights. These investigations indicate that Lucas Heights is located in a zone dominated by low amplitude folding and normal faults. Thus, the LSC is located in a different tectonic domain from the RRR site, which is in a domain in which structures mainly formed during opening of the Tasman Sea.

4.3.1 Fault data in the Sydney region

Faults with throws of up to 100 m are observed throughout the Sydney Basin. These faults typically have steep dips (>60°) and typically strike to the northwest (c. 135°) and the north-northeast (c. 010°) (e.g., Bowman, 1974; Shepherd & Huntington, 1981; Norman & Creasey, 1985; Sherwin & Holmes, 1986; Lohe et al., 1992; Memarian & Fergusson, 1994; Creasey & Huntington, 1985). Fault sets that strike northeast (c. 040°), east (c. 090°) and west-northwest (c. 110°) are also present but in numerical terms are of secondary importance on a regional scale.

Detailed analysis of faults from the Southern Coalfield (south of the RRR site) and from tunnels excavated within Hawkesbury Sandstone (north of the RRR site) indicate predominantly net normal fault displacements on two main sets which strike approximately northwest and north to north-northeast. In addition, some northwest striking faults appear to have experienced late-stage strike slip movements. The northwest striking faults are regional structures with typical trace lengths of 5 to >10 km and maximum apparent throws of 25 to 90 m (Lohe et al., 1992). By contrast there is a tendency for faults striking north-northeast to have displacements of less than 15m. Therefore, in displacement terms northwest striking faults form the dominant set.

The Southern Coalfield encompasses the southern section of the Sydney Basin south of Botany Bay. Fault data in this region were derived from coalmine plans on the top of the Bulli Seam and are two-dimensional. The pattern of faulting for a 10 x 25 km portion of the Southern Coalfield is shown in Figure 4.2**.** The spacings of regional faults in this set are typically 1-3 km. The more northerly striking fault set is dominated by two clustered fault arrays, which are spaced at 3-4 km (Figure 4.1). The Wollongong – Port Hacking 1:100,000 Geological Sheet, which includes the RRR site, shows that there is a tendency for faults striking north-northeast to have displacements of less than 15m, whereas faults striking west-northwest and northwest can locally reach 100 m in displacement (Sherwin & Holmes, 1986). The northwest striking faults appear to have accommodated the highest displacements and can be regarded to be the dominant structures in the Southern Coalfield.

Some of the most complete fault data in the Sydney region are from tunnels that, on the scale of the basin, produce one-dimensional samples of the fault population. Data were examined from six tunnels located north of the RRR site and trending in east-west (five tunnels) and north-south (one tunnel) directions (Figure 4.3). A total of 133 faults were recorded in all tunnels with the main fault strikes being approximately north to northeast and northwest. Approximately 128 of the faults have net normal displacement and only 5 faults appear to have reverse displacement. Displacements range up to 9m with most faults (n=110) having ≤1 m. From our treatment of clustered faults and using the spacing of faults independent of their strike we calculate an average normal fault spacing of c. 140 m. This value increases to 175 m if we consider only faults with a north to northeast strike and increases to 250 m for faults with northwest strike when the obliquity between the tunnel trend and fault strike is accounted for. These results appear to be independent of tunnel trend.

Within the coastal zone some faults appear to have experienced several phases of movement. In some cases fault-slip directions appear to have been reversed resulting in inversion of the net displacement direction. This inversion typically occurs where early normal faults experienced late-stage reverse faulting (Shepherd & Huntington, 1981; Norman & Creasey, 1985; Lohe et al., 1992; Shepherd pers. comm., 2002). The timing of these episodes of faulting is poorly constrained. Many normal faults and dyke systems are inferred to have formed during extension associated with rifting of the Tasman Sea at 83-53 million years before present (Sdrolias et al., 2001). If this is the case then shortening and reverse faults, which typically post-date normal faulting, have been active in the past 53 million years. The upper part of the sedimentary section, presumed to be Tertiary in age is not significantly disrupted by faulting (Colwell et al., 1993) which suggests that the majority of faulting observed in Mesozoic strata predate formation of these Tertiary rocks. Reactivation of N-NE striking normal faults as reverse faults would be consistent with the subsequent east-west contraction (Denham et al., 1981; Denham & Windsor, 1991).

4.4 CONCLUSIONS ON THE REGIONAL GEOLOGY

1. There is extensive data on the geology and seismology of the Sydney Basin.
2. Widespread faulting has been observed throughout the region and mapped extensively in the coal mines and as part of tunnel data for new roads and water/sewage transport channels.
3. The two main fault directions in the region are northwest and north-northeast. In displacement terms, the northwest striking faults are the dominant set. The fault strands on the RRR site belong to the north-northeast set.
4. Normal faults have been seen, on average, every 140 metres in the tunnel data and apparently reverse faults every 1-3 km. These sets of faults have generally small displacements (less than 15 metres).
5. The geology and fault characteristics of the RRR site are consistent with the general pattern of extensive faulting that persists in the local region, a region of low tectonic activity.

5 RESULTS OF THE NEAR FIELD STUDY

The near field study presents the results of a desk study and field reconnaissance of an area within 5 km of the RRR site (Nicol et al, 2002). Fault and lineament data, compiled from rock exposures (i.e. road cuttings, natural exposures along tributaries of the Woronora River, and quarry walls) were examined in an area up to 5 km from the RRR site. Existing data were compiled from Sherwin & Holmes (1986) and from available Coffey's reports. Fieldwork was carried out following completion of the desk study that included an aerial photographic interpretation of available colour aerial photographs.

The rock exposure, access to these rocks and topographic relief are variable. Despite sampling problems introduced by this variability, three faults were located (see table 5.1). Occupying approximately one half of this area, and located to the west of Heathcote Road and the Woronora River, is the undeveloped natural bushland of the Holsworthy Army Reserve, approximately half of which is designated as a "No Go Area" due to the possible presence of unexploded ordnances. The topography of this area is characterised by deeply incised creeks, located between gently sloping ridge areas that are often accessible by four wheel drive tracks.

The eastern approximate quarter of the study area, generally to the east of the Woronora River and west of the Illawarra Railway on more gently sloping land, has been extensively developed for residential purposes.

The remaining quarter of the study area, bounded by Heathcote Road to the west and New Illawarra Road to the east, consists of a number of former quarries, the extensive Lucas Heights Landfill site, and areas of both partially developed and undeveloped bushland.

Three igneous dykes are shown on the 1:100,000 Wollongong-Port Hacking Geological Sheet to the west and north of the RRR site, striking north-northeast. The dyke closest to the RRR site is approximately 200 m to the west of it and strikes 013° with a trace length of 1.2km. The location and existence of this dyke was confirmed by trenching up to 200 m west of the site. A second dyke is located 2.3 km to the north, strikes approximately 025° and extends over a length of 2.8

km. The third dyke is 2.5 km to the northwest of the site, strikes at 020° and has a trace length of approximately 1 km.

No faults are recorded on the 1:100,000 Wollongong-Port Hacking Geological Sheet within a 5 km radius of the RRR site. Geological investigations at the RRR site and immediately surrounding region clearly demonstrate, however, that faults with throws of at least 1 m exist but were not recorded on the map. These faults are too small to be routinely detected and mapped at a 1:100 000 scale.

5.1 OBSERVED FAULTS

The field investigations of a number of identified areas did not reveal the presence of faults where surficial materials were preserved. Therefore, it was not possible to constrain the timing of the most-recent movement. Three minor faults in weathered rock, with vertical displacements of less than approximately 0.3m were observed at three locations within the study area. These faults are described in Table 5.1 below.

Table 5.1 Description of faults observed during near-field study

Site No.	Co-ordinates E	N	Location	Observations
A	316441	6227025	In 4m high rail cutting, 30m south of Wilson Pde road bridge, Heathcote.	Fault in weathered shale, with 0.1m displacement down to north, strike 075°, dip 45°N (i.e. normal separation). No evidence of fault extending to surface, traceable for up-dip distance of approx. 1.5m.
B	313234	6229734	In 8m high road cut on Heathcote Road	Fault displacing a 100mm thick siltstone band by 0.3m, down to east in moderately weathered sandstone. Fault strike 025° (ie NE), dip 80°E (ie. normal separation). No evidence of surface displacement
C	315714	6232683	In disused gravel pit to west of New Illawarra Road, opposite Australia Road	Possible fault in weathered shale near base of 6m deep gravel pit, with 0.3m displacement down to west (ie. normal separation). Strike 350° (ie N-NW), dip 75°W

Note: The co-ordinates given above were obtained from a hand held GPS instrument, and are relative to Australian Mapping Grid (AMG).). The co-ordinates grid used in Figure 5.2 is the Mapping Grid Australia (MGA) system. The AMG and MGA co-ordinates systems are different and cannot be compared directly..

Apart from Site A, the faults noted above tend to be sub-parallel to the two major joint sets observed in the study area, and in the Sydney Metropolitan Area.

During the fieldwork for this 5 km study, close attention was given to locating possible exposures of a dyke reported some 200m west and to the north of the RRR site to examine the possibility that dyke emplacement may have occurred in the path of a previous fault. However, no exposures of the dyke were observed at that time. Later investigations found dykes on the reactor site, west of the footprint for the reactor building.

Figure 5.1 is the map from Sherwin and Holmes (1986) and an expanded and updated version of the local area is in Figure 5.2.

5.2 CONCLUSIONS FROM THE NEAR FIELD STUDY

The conclusions from the 5 km radius study were that:

- Field reconnaissance of accessible soil and rock exposures within 5 km of the RRR site, revealed a few small-scale normal faults with displacements less than 0.3m.
- None of these faults displaces soils and near-surface material. There is no evidence that these faults are active and pose an earthquake hazard for the RRR site.

6 ASSESSMENT AND MAPPING OF THE SITE AND EXCAVATIONS

The second part of the seismic assessment was designed to document fractures (i.e. faults and joints) in rocks exposed in road batters and in the foundation excavation of the Reactor and Neutron Guide Halls at the RRR site (Nicol al, 2002). Fieldwork for this part of the investigation, referred to as Task 2 was completed between April and June, 2002.

The main focus of the investigation was to record fractures in bedrock exposures at the site. The locations, orientations, cross-cutting relationships of fractures together with fault-slip directions were recorded by photographing exposed rock faces and by gridding and logging, mainly at 1:50 scale, faults exposed in the Reactor and Neutron Guide Hall excavations, by surveying the position of fractures in the road batters and by measuring their orientations.

At the RRR site, faults and joints have been discriminated and were mapped separately. Faults are fractures with shear displacement while joints have no demonstrable shear displacement. Fractures are identified as faults when they satisfied at least one of three criteria. These criteria are that faults show; 1) offset or displacement of bedding surfaces or other fractures, 2) shear planes and/or clay gouge along the discontinuity plane, and 3) slickenside striations on the discontinuity plane.

Detailed geological mapping of the RRR site led to the identification, measurement and analysis of 189 joints and faults within the Hawkesbury Sandstone Formation.

6.1 FAULT DATA

Fault strands were identified in bedrock exposures on the RRR site (Figure 6.1). These generally strike to the north-northeast (000-020°), dip steeply (mostly 65-80° east and west) and range in dip separation from 5 mm to 1.3 m (Nicol et al. 2002). The fault strands have both normal and apparently reverse separations that are present in approximately equal proportions and have the same strike. The population of sampled faults is dominated by two fault strands with dip separations of c. 1-1.3 m (the eastern strand) and c. 0.20-0.32 m (the western strand), which are seen in the reactor excavations. A number of the smaller faults are clustered around these dominant structures. Small faults (dip separations 1-8 cm) are also concentrated along the western internal road batter (Figure 6.1).

For the purposes of this report each of the two principal fault strands is described separately, although these fault strands merge at the northern end of the site and appear to constitute strands of a single fault.

6.1.1 Eastern fault strand

In net displacement terms, the eastern fault strand is an apparent normal fault and is the largest fault trace observed at the RRR site (Figure 6.2). The fault extends for at least 140 m across the site in a north-northeast direction (mean strike 013°) and dips steeply to the east (mean dip 67°). Within the area comprising the footprint for the Reactor Building, the fault has a constant dip separation of c. 1-1.3 m up through the rock sequence and across the excavation (N.B. beyond the footprint for the Reactor Building dip separations are probably not complete and cannot be compared directly with the footprint for the Reactor Building data).

The fault geometry changes along its length. South of the footprint for the Reactor Building the fault comprises two main strands in the crane excavation (Figure 6.3; N.B. only one strand was located in the southern road batter and trench but bedding is too discontinuous here to be certain that additional strands have not been overlooked). Northwards from the crane excavation the two fault strands merge into one before reaching the south wall of the footprint for the Reactor Building. In the south wall of the footprint for the Reactor Building the fault has a single main slip surface (Figure 6.4), however, it breaks up into three main strands in the floor of this excavation. These three fault strands were mapped up the north wall of the footprint for the Reactor Building (Figure 6.5) and merge to the north only to bifurcate again towards the northern limit of our mapping (Figure 6.6). At the northern limit of the fault mapping, the eastern fault strand converges with the western fault strand. The intersection zone of the two faults is characterised by a number of joints and faults. Collectively these data indicate that along the length of the eastern fault, strands form an anastomosing network with individual strands of limited lateral extent. One possibly reverse feature with associated folding was observed on the bench in the south wall of the footprint for the Reactor Building.

The fault zone typically consists of clay-rich shears that are commonly associated with iron oxidation or bound soft white material which has been altered. The width of the fault zone varies from 5-10 cm (shears only) to 50-60 cm where white material results from previous geochemical alteration. The fault zone is widest where the primary fault strands intersect and where the orientation of the fault changes locally. Irregularities in the fault surface were observed where it is intersected by prominent cross beds.

6.1.2 Western fault strand

In net displacement terms the western fault strand is the second largest structure observed at the RRR site and has apparent displacement in an opposite direction to the normal fault (Figure 6.7a and 6.7b). This fault trace extends for at least 120 m across the site in a north-northeast direction (mean strike 009°) and dips steeply to the east. The fault was not located south of the footprint for the Reactor Building in a trench excavated to expose the southward projection of the fault. It is probable that the fault extension is covered by a storm water drain. Within the area for the footprint for the Reactor Building the fault has a dip separation of 0.25-0.30 m which changes little up through the rock sequence and across the excavation.

In detail the fault geometry changes along its length. On the south wall of the excavation for the Reactor Building the fault comprises a single fault slip surface (Figure 6.8). The fault bifurcates into two main strands in the floor of this excavation as it approaches the north wall. In the north wall of the footprint for the Reactor Building the fault comprises multiple slip surfaces which broadly step to the east as they pass up through the rock strata (Figure 6.9). This stepping occurs at a bend in the fault and is associated with a west dipping fault strand which connects east-dipping parts of the fault system. The fault strands merge at the top of the north wall and comprise a single slip surface across the southernmost 40 m of the footprint of the Neutron Guide Hall. The fault branches into multiple strands towards the northern limit of our mapping. These strands form a complex zone of faulting and fracturing where the eastern and western strands merge.

The width of the zone of fracturing and minor faulting around the primary fault-slip surfaces varies both along the fault strike and up through the rock sequence. The highest density of secondary joints and faults occurs in the north wall of the footprint for the Reactor Building where multiple primary fault-slip surfaces are present and also where the eastern and western strands converge to the north. These secondary features are generally parallel to the main slip surfaces and are commonly small faults with less than 5 cm reverse and normal displacement. The high density of fractures in the north wall may arise due to a 10 to 20° change in fault strike which occurs on this part of the fault.

The main fault slip surface is typically 1-4 mm wide and marked by a thin white seam. This seam may be accompanied by local iron oxidation but contains little clay material.

6.2 JOINTS

Joints were observed throughout the RRR site where they are commonly highlighted by iron oxidation and brown carbonaceous material. Orientations, lengths and spacings were measured for a total of 172 joints. These measured joints are generally representative of the orientations of the total data set. Joints commonly strike north-northeast to northeast (010°-040°) and dip steeply (>65°).

At numerous localities joints occur in dense clusters with joint-normal spacings of 5 cm to 1 m (Figure 6.10). In these cases joints with the smallest spacings are generally part of the main fracture set (strike 010°-040°).

6.3 CONCLUSIONS ON FAULT MAPPING

1) Geological mapping of the RRR site has led to the identification of two main fault strands within the Hawkesbury Sandstone Formation bedrock that converge in the northern part of the site to form a single fault zone. Both fault strands cross the excavations for the Reactor Building.
2) The two fault strands respectively offset sandstone and mudstone beds by about 1.0-1.3 m and 0.20-0.32 m, and have been traced for 120-140 m across part of the site in a north to north-northeast direction.

7 INTERPRETATION OF THE FAULT DATA

The data described in the previous section motivated additional investigations of the faulting patterns to determine their relevance for the construction of the RRR. Several consultants examined the information and two alternative interpretations have been proposed.

1. In the first interpretation both the eastern and western strands were formed during the opening of the Tasman sea i.e. 53-83 million years ago, and inhomogeneity in the strata or the stress field influenced the nature of the movement on the western strand. This hypothesis is supported by two main arguments. First, the fault plane dips at a somewhat steeper angle than would be expected for a true reverse fault. Second, and more important, the exposure of the same fault on the north face of the main excavation is normal in character and downthrown to the west. Further a series of small dykes up to approximately 0.5 m width occur to the west of the main excavation, which predate any potential fault movement (Gleadow et al. 2002). The dykes occupy a set of fractures that have a similar orientation to the faulting in the excavations and do not appear to have seen any significant disruption.

2. In the second interpretation, the eastern and western strands are part of a system that initiated as a normal fault system, formed during the Tasman Sea opening 83-53 million years ago, with reverse reactivation occurring on one of the strands, and possibly both. This is the most conservative explanation because the reactivation is inferred to have occurred more recently than the Tasman Sea opening.

The first interpretation would immediately render the faulting as not capable (see Sections 7.1 and 9), because any movement would have occurred between 83 and 53 million years ago. Such faulting is typical of the vast majority of the faults in the Hawkesbury Sandstone, particularly within approximately 10 km of the coast.

The second interpretation suggests that the reactivation occurred sometime after 83-53 million years ago. Hence further analysis performed for this report has been performed to test this conservative assumption and to date movements on the western strand using both numerical and relative modern dating methods.

7.1 BASES FOR ASSESSMENT OF THE FAULTS

In reaching conclusions on the suitability of the site for the RRR one can draw on guidelines or criteria for assessment issued by various regulatory authorities. In doing so, it must be noted that available guidelines and criteria are intended for application to the siting of nuclear power plants, not research reactors. The key criterion is whether a fault is 'capable' i.e whether the fault has significant potential for relative displacement at or near the ground surface. The two main sets of criteria, are those from the US Nuclear Regulatory Commission (NRC) and the International Atomic Energy Agency (IAEA). These are used in the comparison in section 9, but both require information to estimate the minimum age of the last movement of any fault.

8 INVESTIGATION OF THE AGE OF THE GEOLOGICAL FAULTS

Two approaches were used to constrain the age of the faulting in the foundation excavation for the RRR. One was to find and date material from the fault itself. The second was to trace the fault to an area where there was overlying material that could be studied, both in terms of geomorphology and for dating purposes, and to make assessments of material in the dykes. A number of trenches were dug to trace the fault across the site and a trench was dug to the north of the site, where the fault was evident in the bedrock and where the younger overlying material was clearly not affected by the fault. This trench is known as Trench 4. Figure 8.1 shows the mapping made of the trench and the various layers that were examined.

Determining the age of rocks or geological events can be done by either numerical-age, relative-age or correlated-age dating techniques. Numerical-age dating directly assesses the age of a mineral/rock (say 10,000 ± 500 years old). Relative- and correlated-age methods provide an estimate of the rock/event age at a site based on correlation with similar features of known age at a different site (e.g. younger than an intrusive dolerite, dated elsewhere to be 10,000 ± 500 years), or based on correlation to an independent time-scale (e.g. magnetic signature relative to known paleomagnetic history of the earth).

A wide range of possible dating methods was considered, summarised in Figure 8.2. The choice depends on the types of material that are available either in the fault itself or in the cover material above the fault. For this study, both direct numerical dating and relative dating methods were used. These included:

- Study of the geomorphology and geochronology of the material in Trench 4. This might indicate the timing of the deposition of the younger, un-faulted sediment overlying the fault. The conclusions are discussed in Section 8.1.
- Optically stimulated luminescence (OSL) to date the unfaulted strata that overlie the fault in trench 4. This is reported in section 8.2.
- Paleomagnetic dating using the magnetic signature of the rocks and relating that to the information known on magnetic reversals and on movements of the earth's magnetic pole.

This was done both for material crossing the fault and with samples taken at various locations in Trench 4. Results are given in section 8.3.

- Fission track and (U-Th)/He dating. Such dating of detrital apatites from the sandstones would provide information on the timing of deep erosion of the area, also setting a younger limit on the timing of fault movement. The results should constrain the total depth and timing of deep erosion which has occurred over the area and provide another minimum age estimate for the time of faulting. These results are discussed later.

8.1 LOCATION AND DESCRIPTION OF TRENCH 4

Trench 4 was excavated outside the main perimeter fence along the northward projection of the eastern and western fault strands mapped across the construction site. The trench was excavated in late July and logged in early August, 2002. The purpose of this trench was to determine the location, geometry, and displacements of the faults in bedrock immediately north of the RRR site and to analyse the age relations of fault movements and deposition of up to 2 m of probable Quaternary deposits which overlie the bedrock. In addition, as the eastern and western fault strands converge in the area of the footprint for the Neutron Guide Hall, it is useful to consider their relationship to one another in an area where they should have merged to form one fault.

In order to assess the minimum age of faulting, it is necessary to view the relations between faulting in bedrock and the stratified sequence within 2 m of the ground surface. If, in these circumstances, Quaternary deposits are not displaced by faulting, then the age of these deposits provides a minimum age for the last fault-movement event.

The footprint for the Reactor Building at the RRR site is located atop a relative high point (ridge) in broadly undulating topography. From the footprint for the Reactor Building the site slopes gently downwards at c. 8° to the northeast and towards Trench 4, which is located in a broad shallow gully. The altitude of the Reactor and Neutron Guide Halls prior to the commencement of construction was c. 154-157 metres, while the ground surface at Trench 4 is at an altitude of c. 150 m (Figure 8.3). Immediately beyond the RRR site these gentle slopes continue to decline in all directions except to the south and southwest where altitude decreases rapidly down a steep sandstone gully and escarpment.

At the RRR site, the probable Quaternary cover deposits were eroded prior to the commencement of geological investigations. In all likelihood the unmodified cover on the RRR site would have been thin because ridges are typically erosional rather than depositional environments. Erosion usually dominates on ridges as these high areas lack a source area for sedimentation and because *in situ* soils and bedrock weathering products tend to be transported down-slope from high points in the topography. The most likely local accumulations on ridges during the Quaternary are bedrock-weathering products which develop into lateritic soils. These soils may form during warmer and wetter periods (Interglacial periods) and be stripped off during colder, dryer periods (Glacials) and so the overall accumulation of Quaternary products can be expected to be minor.

Reconnaissance geologic investigations of the site and immediately surrounding area (i.e. within 100m of its perimeter fence) revealed a prospective location for trenching across the projected position of the main faults c. 50 metres north of the perimeter fence. Trench 4 was excavated here and is located in a wooded area between Old Illawarra Road and New Illawarra Road. This site is in a broad gully and a trench was considered likely to contain Quaternary deposits undisturbed by human activity, with which the faulting assessment could proceed.

8.1.1 Stratigraphy

The floor of Trench 4 is within Hawkesbury Sandstone bedrock, which here comprises massive to cross-bedded, quartz sandstones of medium to coarse grain-size. Hawkesbury Sandstone extends up c. 3 metres above the trench floor. These sandstone beds increase in their weathering toward the ground surface, losing their cementation. Slightly weathered Hawkesbury Sandstone is exposed at the base of the pit. Saprolite (in situ weathered rock) occurs over the bedrock. Within the bedrock, faulting is localised in a zone that is 5 metres wide and located at the eastern end. A zone of dense ferruginous iron cementation marked by purple discolouration of the rock occurs within sandstone beds west of the faults. Six samples (PM 1-6) were collected by Dr B Pillans of the Australian National University (ANU) for paleomagnetic analysis, to determine the timing of formation of this oxidised cement. The weathered top of the bedrock grades into weathered colluvial cover deposits (Unit 3) above it (Figure 8.1). The location of the change from bedrock to colluvium is defined by a "stone-line"of iron-cemented clasts (above Bench 2; Figure 8.1). Four of these clasts (PM 7-10) were sampled for paleomagnetic orientation.

The stratigraphy of Trench 4 is shown in Figure 8.1 and comprises 5 main units (1-5). Unit 3 is the lowermost unit and rests on bedrock. It consists of a 1 metre thick grey mottled sand bed that contains a number of thin concretion or nodular horizons, intense iron (red) mottling, and a series of vertical, clean bleached well-sorted coarse quartz sand-filled pipes, which merge to form a polygonal network in planview. This unit may be composed of a least 2 separate sand-sheets (not shown on log), representing distinct episodes of deposition. The material comprising Unit 3 appears to have been transported to the trench site, rather than accumulating *in situ*, and is probably of colluvial, aeolian, or alluvial origin. At this time it is, however, uncertain whether Unit 3 formed due to the gradual accumulation of material, or whether it formed during punctuated periods of relatively rapid sedimentation. Unit 3 is likely to be of Quaternary age.

Overlying Unit 3 are two planar late Quaternary horizons (Units 1 and 2) and two young infilled channels (channels 1 and 2). Unit 2, which immediately overlies Unit 3, is a grey-brown massive fine sand, with a thin paleosol A horizon in its upper 10 cm. Unit 2 is free of iron-rich mottling. One OSL sample was taken from the basal contact of Unit 2 with Unit 3. Unit 1 is a fine white sand that extends up to the ground surface where it is not truncated by the younger channels. This (approx. 5cm) medium-brown soil has formed on this unit. The presence of paleosols on top of Units 1 and 2 may suggest that the formation of these units was followed by a significant period of time (e.g. >10,000 years) when no deposition or erosion occurred. The sedimentary process that deposited Units 2 and 3 is again uncertain, but as with Unit 3, was probably colluvial in nature.

The regolith above the bedrock is not, in any way, displaced by the fault movement in the bedrock. It is certain that fault movement has not occurred since the deposition of the alluvium and colluvium (Unit 3), and it is likely that there has been no movement since the formation of the saprolite (the lowest layer above the bedrock).

8.2 LUMINESCENCE DATING

Daylight releases charge from light-sensitive traps in defects in quartz crystals, a process commonly referred to as bleaching (Aitken, 1998). Optically stimulated luminescence (OSL) can be used to estimate the burial age of sediments because when grains of quartz are buried they accumulate a trapped-charge population due to the effects of ionizing radiation from the surrounding environment, and this trapped-charge population increases with burial time (Huntley et al., 1985). The time elapsed since burial can be determined by first measuring the OSL signal and determining the equivalent-dose (D_E), and then by dividing this parameter by the time-averaged flux of ionizing radiation dose (the dose-rate). Optical dating has been widely used by Quaternary researchers for over fifteen years, and is widely accepted as a viable chronological tool by the scientific community (e.g. Murray and Olley, 2002). The age range of optical dating of quartz grains varies considerably, and depends on both the dose-rate and the intrinsic saturation dose of the quartz sample in question. A typical upper age limit for Australian sedimentary quartz buried in a sediment with an environmental dose-rate of around 1 Gy/ka might be of the order 150 ka.

Where sediments deposited within the age range of optical dating display evidence of tectonic activity, the burial age of the quartz grains yields a maximum age for the tectonic activity. Where OSL dated sediments that are beyond the age range of optical dating do not exhibit any evidence of tectonic activity, the dates provide a minimum age for tectonic activity that may have occurred in geological units underlying the sediment in question. The investigations into the timing of tectonic activity at Lucas Heights fall into this category.

8.2.1 Dating Methods

Samples for optical dating were collected in the field by inserting light-proof 0.3 m lengths of PVC into sediments exposed by trench excavations. Samples were then transported to a red-light laboratory at Melbourne University for all further analysis.

Table 8.3 Optical ages and dose rates

OSL sample[1]	Water content (%)[2]	D_E (Gy)	Total dose rate (Gy/ka)	K (Bq/kg)	U (Bq/kg)	Th (Bq/kg)	Cosmic-ray dose rate (Gy/ka)[3]	Age (ka)
0222-02: 0.4m	5.4	16.6 ± 0.5	1.18 ± 0.04	36 ± 3	15.8 ± 0.2	29.3 ± 0.6	0.20 ± 0.02	14 ± 2
0222-01: 0.6m	5.5	25.7 ± 1.1	1.18 ± 0.04	44 ± 3	16.7 ± 0.2	27.6 ± 0.6	0.19 ± 0.02	22 ± 3
0222-04: 0.8m	5.8	46 ± 5	1.72 ± 0.06	67 ± 8	21.9 ± 0.4	48.1 ± 0.4	0.18 ± 0.02	27 ± 4
0222-05: 1.1m	5.5	95 ± 10	1.78 ± 0.06	50 ± 9	24.2 ± 0.4	52.1 ± 0.4	0.17 ± 0.02	53 ± 6
0222-03: 1.5m	6.3	>170	1.64 ± 0.06	30 ± 11	21.1 ± 0.4	51.7 ± 0.4	0.16 ± 0.02	>104

All errors are 1σ.
1. *Sample locations and stratigraphic units are shown in Fig. 8.1.*

Samples 0222-02: 0.4m (14 ± 2 ka) and 0222-01: 0.6m (22 ± 3 ka) (refer Figure 8.1) were taken from homogenous grey/brown sands. These sands form an extensive near surface layer across the site, and were probably deposited by wind between 14 and 22 ka.

The remaining samples were taken from mottled brown sands from 0.8 to 1.5 m depth. The apparent depositional ages of these samples increase exponentially with burial depth, which is characteristic of a bioturbated soil, in which floral/faunal processes have transported recently bleached grains from the surface down into the soil profile. Exponential decreases in bioturbation process with depth have been previously documented (e.g. Humphreys and Field, 1998). Therefore it is concluded that the average luminescence ages are likely to be comprised of some grains that have not been exposed to sunlight for millions of years and have saturated luminescence signals, some that have been exposed to sunlight relatively recently. No attempt was made to quantitatively unravel rates of surface-to-depth bioturbation or mixing processes. The oldest age of >104 ka occurs at a depth of 1.5 m. Below 1.5 m, the quartz luminescence signal is saturated, which means that the grains last saw sunlight before 104 ka. The luminescence ages cannot be used to ascertain whether the mottled sands are derived from in-situ weathering and bioturbation of the underlying sandstone, or whether they are derived from hill-slope depositional processes.

There is no evidence for displacement along the interface between the *in-situ* sandstone and the overlying mottled layer sands, nor is there any evidence that fault planes propagate through the mottled zone.

8.3 PALEOMAGNETISM

The formation of secondary iron-oxides by chemical weathering processes provides a means to apply paleomagnetic techniques to date regolith materials. A Chemical Remanent Magnetisation (CRM), aligned with the Earth's magnetic field, may be acquired by mineral grains either during nucleation and growth through a critical blocking diameter (single phase CRM forming magnetite), or during alteration of an existing mineral (two phase, or parent-daughter CRM) e.g during weathering. Hematite (αFe_2O_3), a commonly formed secondary mineral in oxidising conditions, is a stable magnetic remanence carrier in its closely related form maghemite. Therefore, the magnetic remanence in weathered regolith relates to the time of formation of magnetite and maghemite.

The ages of weathering-induced magnetisations are obtained in two main ways:

1. By using the Geomagnetic Polarity Time Scale (GPTS). The polarity of Earth's magnetic field over the last 780,000 years has generally been the same as it is now (referred to as "normal" polarity), but prior to that, there was a long interval (back to 2.6 million years) of dominantly opposite or "reversed" polarity (Figure 8.3), and prior to that, numerous other normal and reversed polarity intervals (e.g. Opdyke & Channell 1996). Short intervals of reversed polarity of up to a few thousand years have been reported in the Brunhes Normal Chron (e.g. Jacobs 1994). However, CRM's are acquired over long enough intervals that such short-term field changes are not recorded. The last 780,000 years is named the Brunhes Normal Chron, and the reversed interval before that is named the Matuyama Reversed Chron. The Brunhes/Matuyama polarity transition (B/M transition), dated at 780,000 years by precise $^{40}Ar/^{39}Ar$ dating of volcanic rocks (e.g. Spell & McDougall 1992) and astronomical calibration of deep sea core stratigraphies (Shackleton et al. 1990), is used as a major chronostratigraphic marker in Australian regolith studies (Pillans & Bourman 1996). Typically, magnetostratigraphy is best used for dating sedimentary sequences, preferably with some independent age control from other dating techniques. However, reverse polarity CRM's predates 780,000 years, and as such can provide a useful minimum age in regolith materials (Pillans & Bourman 1995).

2. By comparison with the Australian Apparent Polar Wander Path (AAPWP). An important characteristic of most CRM's is that they are acquired over long enough times (thousands of years) to average out secular variation of the geomagnetic field. Thus paleomagnetic poles can be calculated from the remanence directions, which in turn can be used to derive weathering ages by comparison with paleomagnetic poles of known age (a trajectory of such poles is usually referred to as the apparent polar wander path). This approach is particularly useful in Australian regolith studies, because the continent has substantially changed its latitudinal position during the Tertiary and Quaternary as a result of plate motion. The Australian Apparent Polar Wander Path (AAPWP) for the last 100 million years is shown in Figure 8.4.

Rocks exposed in excavations at Lucas Heights have been weathered in the past, with zones of red-brown ferruginization evident to depths of several metres. The ferruginized zones have generally smooth, sharp boundaries with surrounding pallid areas. Structural and bedding control of the colour patterns is evident – pallid zones tend to follow joints and faults, suggesting that iron mobilisation post-dates the joints and faults, which also acted as conduits for water movement and controlled oxidation-reduction reactions.

8.3.1 Sampling

Oriented block samples (typically about 10x10x20 cm in size) were collected from exposures in Trench 4, 5 and 6 and the reactor excavation site. Four major types of ferruginous materials were sampled.

- Group 1: Red-brown zones of oxidised bedrock (sample numbers PM14, 15, 16, 23, 24 from across the area where the fault strands merge in the northern end of the site).
- Group 2: A ferruginous layer in the south wall of the reactor building excavation (Figures 6.7a and 6.7b), which crosses both faults and post-dates fault movement (sample numbers PM11, 12, 13, 17, 18, 19, 20, 21, 22), since it is not displaced by the fault.
- Group 3: Red-brown zones of oxidised bedrock (sample numbers PM1-6 from the undisturbed layers in Trench 4).
- Group 4: Clasts of oxidised bedrock in Trench 4, which appear to occur immediately above an unconformable contact between *in situ* bedrock, and overlying transported cover (sample numbers PM7, 8, 9, 10).

Initially, samples were field oriented using a Brunton magnetic field compass. However, after laboratory analysis, several samples from the south wall of the reactor pit yielded anomalous results. Field checking on 6/09/2002 showed discrepancies between sun compass and magnetic compass declinations, caused by magnetic field anomalies close to steel construction materials. All other samples showed close agreement between magnetic and sun compass declinations. Sun compass values were used for recalculating field orientation of previously collected samples, and also for orienting new samples.

8.3.2 Results and discussion

The presence of reverse polarity CRM's in the majority of specimens from the oxidised zones, and in all specimens in the ferruginous layer, clearly indicates remanence acquisition prior to the B/M transition at 780,000 years. Since the formation of the ferruginous layer post-dates fault movement, the fault has not sustained surface rupture for at least 780,000 years.

The reverse polarity CRM's could have formed during any one of the many intervals of reversed polarity prior to the B/M transition. Paleomagnetic poles may be used to further constrain the age.

The paleomagnetic pole from Group 1 specimens (Fig. 8.4) is statistically indistinguishable from that expected for the Matuyama reversed Chron (2.6 to 0.78 million years).

Pillans & Bourman (2001) demonstrated, using magnetostratigraphy, that a marked shift in climate occurred in southern Australia in the early Brunhes Chron. The arid shift resulted in a marked change from lacustrine to saline conditions, accompanied by increased dust fluxes, and a change from oxide-dominated weathering regimes to carbonate-dominated weathering regimes in the Adelaide region. The pervasive mobilisation of iron oxides at Lucas Heights, predating the B/M transition, is consistent with widespread formation of hematite mottles in the Adelaide region during the Matuyama Chron and the regional paleoclimatic model for southern Australia (Pillans & Bourman 1995, 2001).

The paleomagnetic poles from both Group 2 and Group 3 specimens are statistically significantly different from Group 1 specimens. The 95% confidence limits on these poles, each overlap with the 12 million year old reference pole on the Apparent Polar Wander Path (Figure 8.4). Based on the pole latitudes, an age of 9±4 million years is estimated for Group 2, and 14±8 million years for Group 3.

Specimens from the Group 4 oxidised clasts yield stable magnetisation directions that are neither normal nor reversed. The remanence directions differ from clast to clast, and also differ from the *in situ* bedrock samples. It is therefore concluded that the clasts have been rotated since remanence acquisition.

A synthesis of published and unpublished paleomagnetic studies on weathered regolith in southern Australia (Pillans 2002), shows three major episodes of deep oxidative weathering; Late Tertiary (1.6-20 million years), earliest Tertiary (55-65 million years) and Jurassic (170-180 million years). The episodes are postulated to represent climatically-driven weathering events. Both the Group 1 and 2 poles indicate weathering ages within the Late Tertiary interval. The formation of hematite-rich beds in weathered Hawkesbury Sandstone at Lapstone, western Sydney, is also considered to have occurred during the late Tertiary (Bishop et al. 1982).

8.3.3 Conclusions from paleomagnetic dating

1. Paleomagnetic results from Lucas Heights demonstrate that secondary iron oxides have reverse polarity magnetisations that predate the Brunhes/Matuyama paleomagnetic transition at 780,000 years.
2. A reversely magnetised ferruginous layer in the south wall of the reactor excavation post-dates fault movement. The fault has therefore not moved in the last 780,000 years.
3. The paleomagnetic pole calculated for this unfaulted ferruginous layer crossing the fault yields an age estimate of 5-13 million years old. The fault has therefore not sustained surface rupture for at least the last 5 million years.

8.4 THERMOCHRONOLOGY RESULTS

Professor A Gleadow and associates (Gleadow et al 2002) studied the deep weathering that occurred at the site and analysed the thermochronology of the major depositional periods. They concluded that the most important and robust constraint that can be supported by observations at the site is that all fault movements pre-date the time of the pervasive deep weathering episode. This is firmly constrained by the occurrence of localised zones of bleaching and ferruginous cementation along various fault planes, including the western strand, in the weathered zone exposed in the main excavation. This requires that the fracture planes of the faults were already in existence during the deep weathering process (probably itself an episode of long duration), and have not moved since.

During the geotechnical studies, a number of boreholes were drilled and the cores extracted for analysis. Dating of detrital apatites from sandstones obtained from the deepest (ca 50m) of the test boreholes at the RRR site were studied by both the Fission Track and (U-Th)/He methods (Gleadow et al, 2002b). These are temperature sensitive dating methods, the results of which relate to the time of cooling of the rocks as they approached the near surface environment due to surface denudation.

Nine core samples were examined from depths of between 43 and 51 m in the four deepest test boreholes at the RRR site (BH 106, BH 107, BH 109 and BH 110). Of these nine, three samples were selected for thermochronological study on the basis of the amount of apatite recovered by mineral separation and its suitability for analysis. All samples are from fresh Hawkesbury Sandstone below the deeply weathered layer and sample details are summarised in Table 8.2.

Table 8.2 Thermochronology sample details, Replacement Research Reactor Site

Sample Number	Depth (m)	Lithology
BH 107A	45.0 - 45.38	Laminated micaceous silty fine-grained sandstone with dispersed organic matter
BH 109C	48.15 – 48.55 m	Well-sorted micaceous coarse sandstone with interbedded carbonaceous matter
BH 110B	51.0 – 51.5 m	Micaceous silty fine grained sandstone and laminated silty sandstone with well sorted quartz-rich coarse sand

8.4.1 Fission Track Results

Apatite fission track (AFT) results for the three samples are summarised in Table 8.3 (This table is at the end of the report because of its size). In all cases apatite yields from the samples were excellent with ≥20 apatite grains being counted for age determinations and at least 39 confined track lengths measured. Apparent AFT ages vary from 69±4 million years to 75±4 million years and statistically can be considered to be concordant (within analytical error at the ±2σ level). The observed mean Track Lengths vary from 13.63±0.15 µm to 14.44±0.17 µm. Mean Length distributions are generally unimodal with low to moderate standard deviations.

8.4.2 (U-Th)/He Results

Preliminary estimates were obtained for the (U-Th)/He system in Table 8.4, based on U values from the fission track work. The thorium content is estimated on the basis of a typical Th/U ratio of 5 in continental crustal rocks. On this basis, the errors indicated are estimated at 10% of the helium age.

TABLE 8.4: Preliminary Results of the (U-Th)/He Dating of Apatite

Sample	^{4}He gas volume (ncc)	Mean grain radius (µm)	FT (α.correction)	He – Age (Ma)	Error (Ma)
BH-109A	0.351	29.8	.57	38.4	3.8
BH-109B	0.411	30.4	.56	45.7	4.6
BH-107A-1	0.442	31.3	.60	78.7	7.8
BH-107A-2	1.120	31.3	.61	25.6	2.6

The liberated Helium gas volumes for these samples were of the order of 10 times the background levels, thus providing quantifiable results. Samples BH-109A and BH-109B yield replicate ages (within error) and have a mean helium age of ~ 42 million years. Duplicate samples generally indicate a robust helium age. In contrast, samples BH-107A–1 and BH-

107A–2 failed to replicate. This probably results from the inclusion of a submicroscopic mineral inclusion with a high actinide concentration (eg. zircon or monazite are common). However, the lack of a replicate analysis for both samples means that data for samples BH-107A-1 and BH-107A-2 cannot be considered robust.

8.4.3 Thermal History modelling

Results of thermal history modelling of the fission track data are shown for sample BH109C in Figure 8.5, using the indicative (U-Th)/He results as an additional constraint on the thermal history. Modelling was carried out using the method described by Gallagher et al. (1985) and reveals an episode of rapid cooling between about 85 and 65 million years, followed by a period of much slower cooling. The modelling also conforms with a regional value for vitrinite reflectance of coal particles in the sandstones of R_o=1.0% (summarised by O'Sullivan et al, 1996). These vitrinite reflectance values suggest that the maximum palaeotemperature experienced by the site was around 135°-145°C prior to the commencement of rapid cooling.

The measured helium age is a combination of competing effects of radiogenic ^{4}He in-growth from the decay of actinides (U and Th) and the diffusive losses sustained during prolonged exposure to elevated temperatures in the earth's crust. The mineral apatite readily loses helium at temperatures above ~70C, but retains increasing amounts of the helium production as the mineral cools during exhumation. If a relatively simple cooling history is indicated for the region, then in conjunction with apatite fission track analysis, reasonable estimates can be made for amount of retained helium (ie. the helium age) expected in a sample. This is achieved by means of numerical modelling of the in-growth/diffusion process over the cooling history. Sample BH-109 (A-B) was modelled using the approach of Wolf et al. (1998) and using Ken Farley's (Cal Tech) code. The diffusion parameters of the Durango age standard were input as default estimates for the model. The modelling indicates that a helium age of ~ 42 million years (BH-109 A & B) is consistent with the monotonic cooling of the host rock from a temperature of ~ 75C beginning at around 48 million years ago. If a geothermal gradient of ~ 25C/km is assumed, this would equate to an exhumation rate of approximately 46 m/million years over the last 48 million years.

8.4.4 Interpretation and the evolution of the present land surface

Fission track dating on apatite relates to cooling through the interval 110°-60°C and (U-Th)/He dating to cooling through approximately 80°-40°C, so that it is expected the ages would occur in this relative sequence during a normal cooling pattern. This is exactly what is found for the samples analysed here as can be seen in Tables 8.2 and 8.3 and the results are also consistent with other fission track results from the Sydney Basin reported by O'Sullivan et al (1996) The results from both methods are consistent with a period of rapid cooling being experienced by the sandstones in this area between about 85 and 65 million years. Thereafter, cooling was very slow until the present day, consistent with the establishment of a land-surface of low relief upon which the pervasive deep weathering now observed at the site to a depth of 14-18m was developed.

8.4.5 Relationship to possible fault movements

The relationship of the derived cooling history to the age of faulting is judged to be as follows. First, the rapid cooling between about 80 and 60 million years is due primarily to reduction of surface relief, probably created during continental rifting and opening of the Tasman Sea. This is probably the time of extension movements throughout the basin and is the most likely time of extensional movement on the observed fault. Second, the slow cooling that followed the initial rapid cooling represents the period over which the low-relief plateau surface on which the site is located. This phase culminated in the pervasive deep weathering that is now preserved on this site and similar plateaux sites throughout the Sydney Basin. On the basis of the thermochronology, this period of deep weathering is likely to be no older than about 35 million years and is regarded on geological evidence as being no younger than Miocene in age (Herbert, 1980).

The age of the deep weathering episode provides the most unambiguous constraint on the last possible time of fault movement. It is concluded that this constraint is likely to fall in the interval 35-10 million years.

8.5 Conclusions from Dating

The results presented above provide a consistent picture of the age of the material in the fault and overlying the fault. The OSL data give consistent ages of the overlying Quaternary material that range from 14,000 years in the upper aeolian layers (unit 2 in Trench 4) to greater than 104,000 years in the Unit 3 sand layers (Unit 3) above the fault itself. Nevertheless, there is no evidence that they have been displaced by the fault. Given the fact that this material appears to have been transported to the site and may have been subject to various removal and replacement cycles, these ages are much younger than the fault itself. Both the paleomagnetic analysis of the clasts at the bedrock to cover interface and the geomorphology confirm that the material has been transported to the site and probably replaced several times since the fault developed, and is not simply weathered bedrock.

On the basis of the thermochronology, a consistent picture emerges of the major episodes of movement and deposition. The age of the deep weathering episode, which post-dated the fault movement, provides the most unambiguous constraint on the last possible time of fault movement and gives an interval of 35-10 million years since the last movement.

Paleomagnetic results provide a direct assessment of the limiting age of the most recent movement of the fault itself by linkage to the last magnetic reversal and by location on the polar wander path. These data confirm an age of at least 5 million years since the last movement on the fault, with a mean age of 9 million years. As noted in Section 5, this dating is associated with the most conservative interpretation of the movements in the excavations. Other interpretations would place the age of faulting at the time of Tasman Sea opening, around 83-53 million years.

The results confirm that the last activity on the fault occurred millions of years ago.

9 ASSESSMENT OF THE CAPABILITY OF THE FAULT

In this section the findings of the investigations are compared with the criteria developed by the IAEA and the USNRC, as mentioned in Section 7, to assess the capability of the faulting seen in the RRR site.

9.1 COMPARISON WITH IAEA CRITERIA

The IAEA Safety Guide (50 SG-S1, 1991) sets out criteria for determining capability. The basis for answering such a question should be the database of geological and seismological investigations. Using the IAEA definition, a fault shall be considered capable if:

4. *It shows evidence of past movement or movements of a recurring nature within such a period that it is reasonable to infer that further movement at or near the surface can occur. (In highly active areas, where both earthquake and geological data consistently reveal short earthquake recurrence intervals, periods of the order of tens of thousands of years may be appropriate for the assessment of capable faults. In less active areas, it is likely that much longer periods may be required.)*

As discussed in this report, the most recent fault movement is at least 5 million years old, the thermochronology indicates a minimum of 10 million years, and the fault shows no evidence of past movement or movements of a recurring nature within such a period that it is reasonable to infer that further movement at or near the surface can occur.

5. *A structural relationship has been demonstrated to a known capable fault such that movement of the one may cause movement of the other at or near the surface.*

The nearest known possible Capable Fault to the site fault is the Lapstone Structural Complex located approximately 35 km west of the site. Because of this substantial distance no secondary movement is expected to occur on the site fault. In addition, a considerable amount of geological and geophysical investigation has taken place between the Lapstone Structural Complex and the coast, related to coal and gas exploration. These investigations have proved conclusively that similar zones to the Lapstone Structural Complex do not extend further east towards Lucas Heights. Structural geology considerations also place the Lapstone Structural Complex in a separate tectonic zone, west of the coastal zone in which the site occurs.

6. The maximum potential earthquake associated with a seismogenic structure, as determined in section 4 (*of the IAEA guide*), is sufficiently large and at such a depth that it is reasonable to infer that movement at or near the surface can occur.

The only seismogenic structure is the LSC. The conservative choice for the repeat time for the LSC is 11-27 ka (Alliance 1999 report), so the LSC will have ruptured many times during the past 5-13 million years and clearly has not triggered any slip at the RRR site. That covers triggered slip. At a more elementary level one may also ask about direct co-seismic slip. For this to happen the RRR site fault would need to be part of the same structure as the LSC and clearly it is not.

9.2 COMPARISON WITH USNRC CRITERIA

These data allow evaluation of the fault movement timing with respect to definitions of Capable Faults as used in nuclear power plant siting guidelines. The criteria, as presented by the U.S. Nuclear Regulatory Commission (in press, 2002), are:

i) "*The presence of surface or near-surface deformation of landforms or geologic deposits of a recurring nature within the last, approximately, 500,000 years, or at least once in the last, approximately, 50,000 years.*"

As discussed in this report, the most recent fault movement is at least 5 million years old by paleomagnetic measurements and the thermochronology indicates a minimum of 10 million years.

ii) "*A reasonable association with one or more large earthquakes or sustained earthquake activity that is usually accompanied by significant surface deformation.*"

The site fault has not been associated with a large earthquake or sustained earthquake activity (Alliance 1999).

iii) "*A structural association with a capable tectonic source having characteristics described in Point 1 so that movement on one could be reasonably expected to be accompanied by movement on the other.* "

The nearest known possible Capable Fault to the site fault is the Lapstone Structural Complex located approximately 35 km west of the site. Because of this substantial distance no secondary movement is expected to occur on the site fault. In addition, the Lapstone Structural Complex is located in a separate structural zone to the coastal zone where the RRR site is located.

The PSHA study (Alliance 1999) identified a circa. 10 km distance to a magnitude 5.5-6.5 earthquake as the most likely earthquake to affect the ground motions in a 10,000 year period at the site. This implies such a source could be a Capable Fault if the earthquake had a shallow focal depth. From precedent observations in historical earthquakes at those magnitudes no sympathetic or secondary movements are expected on the site fault.

Therefore, the site fault cannot be classified as Capable by the criteria established by the USNRC or the IAEA for the siting of nuclear power plants.

Therefore, these faults are clearly not potential seismic sources, even under the most conservative assumption on the age of last movement of the fault discovered in the RRR excavation, and they do not pose a surface-fault rupture hazard. This confirms that there is no need to alter the outcomes of the analysis already performed as part of the probabilistic seismic hazard assessment. This analysis considered the appropriate peak ground acceleration and hazard spectrum to be used for the Lucas Heights region, based on the overall seismicity of the region. Given this conclusion, and the conservative nature of the design process, there is no change required to the design hazard spectrum or the facility design, put forward in the PSAR in May 2001.

10 CONSULTANTS AND PEER REVIEW

In performing these additional investigations, ANSTO has engaged a number of experts both nationally and internationally to ensure that the process was thorough, systematic and according to international practice. These consultants were:

1. GNS of New Zealand, who had conducted the probabilistic seismic hazard assessment, under contract to the Department of Industry, Science and Resources, performed the bulk of the site investigations and mapping of the geology and geomorphology of the trenches.
2. F H(Bert) Swan , an internationally respected consulting geologist from California, reviewed the work performed by GNS. He concluded that "*The technical approach and dating methods being used by ANSTO's consultants to assess the age of the faulting at the site are in accordance with the current state-of-the-practice for paleoseismic investigations*".
3. Dr B Pillans, a research scientist from the Australian National University, performed the paleomagnetic dating, reported in section 8.
4. Dr J Shepherd, a principal consulting geologist with extensive experience with the southern coal mines, concluded that "The contents and conclusions of the GNS report in my opinion represent the results of a thorough and high quality survey …. The normal and reverse fault zone passing through the new Research Reactor Site is most probably part of a wider zone of small displacement faults of a relatively minor nature formed a considerable time back in the geological past. Evidence of any more recent movements along the faults is completely lacking. This is also consistent with the extent of knowledge of Sydney Basin fault zones in the Permian and Triassic strata in the coastal areas."
5. Dr G Wilson, from Otago University in NZ and former head of the paleomagnetic laboratory at the University of Oxford, UK peer reviewed the work of Dr Pillans. He confirmed the work of Dr Pillans and concluded that "*The two reversed polarity components of magnetisation indicate two phases of weathering and secondary iron oxide mineral formation in the regolith above the faulted bedrock; the first at 9±4 million years ago and the second at 0.8 – 2.6 million years ago".*
6. J Cramsie, until recently Director of the NSW Geological Survey, provided advice on the local geology and concluded that *"Mapping and other field investigations undertaken by GNS and their associates has been appropriate to the critical issues and of a high standard*".
7. Professor A Gleadow and B Smith of the University of Melbourne performed optically stimulated luminiscence dating, reported in section 8.
8. Professor A Gleadow and associates of the University of Melbourne performed the thermochronology of the borehole cores, reported in section 8.
9. Dr C Pain of Geoscience Australia reviewed the conclusions on the geomorphology of Trench 4 and concluded that "*The pit, and the surrounding landscape, shows landforms and regolith typical of much of the area of Hawkesbury Sandstone where shallow valleys and gentle slopes dominate the landscape. It is clear that there has been no fault movement since the saprolite and overlying sediments began their formation. This means that any dates obtained for these materials will indicate a significantly younger age than any fault movement*".

11 REFERENCES

1. Aitken, M. J. (1998). An introduction to optical dating. The dating of Quaternary sediments by the use of photon-stimulated luminescence. *Oxford University Press, U.K.*
2. Alliance (1999). Seismic hazard analysis of the Lucas Heights site of the High Flux Australian Reactor. *Report to Australian Department of Industry, Science & Resources.*
3. Bembrick, C, Herbert, C, Scheibner, E, Stuntz, J. (1980). Structural subdivision of the Sydney Basin. In: Herbert, C. & Helby, R (editors), A guide to the Sydney Basin. *Department of Mineral Resources, Geological Survey of New South Wales*, *Bulletin* 26, 4-9.
4. Bishop, P., Hunt, P., Schmidt, P. W. (1982). Limits to the age of the Lapstone Moncline, N.S.W. — a palaeomagnetic study. *Journal of the Geological Society of Australia*, 29, 319–326.
5. Bowman, H. N. (1974). Geology of the Wollongong, Kiama, and Robertson 1:50,000 Sheets. *New South Wales Geological Survey, Sydney.*
6. Coffey Partners International Pty Ltd (1998). Replacement Reactor Site, Lucas Heights, Geophysical Study. Report No. GY617/1-AC, April 1998.
7. Coffey Partners International Pty Ltd (1998). Replacement Research Reactor, Lucas Heights, Hydrogeological and Hydrochemical Study. Report No. G459/1-AG, August 1998.
8. Coffey Partners International Pty Ltd (1998). Replacement Research Reactor, Lucas Heights, Geotechnical Investigation. Report No. S10948/1-AF, June 1998.
9. Coffey Geosciences Pty Ltd (1999). Replacement Research Reactor, Lucas Heights, Report on Near Site Investigations. Report No. S20251/1-AQ, October 1999.
10. Coffey Geoscienecs Pty Ltd (1999). Replacement Research Reactor, Lucas Heights, Geotechincal Investigations. Report No. S20251/1-BB, November, 1999.
11. Colwell, J. B., Coffin, M. F., Spencer, R. A. (1993). Structure of the southern New South Wales continental margin, southeastern Australia. *BMR Journal of Australian Geology and Geophysics,* 13, 333-343.
12. Creasey, J. W., Huntington, J. F. (1985). Lineament patterns of the Sydney Basin – An overview. Advances in the study of the Sydney Basin, Proceedings of the nineteenth symposium, *Department of Geology, The University of Newcastle*, 12-14.
13. Denham, D., Weekes, J., Krayshek, C. (1981). Earthquake evidence for compressive stress in southeast Australian crust. *Journal of Geological Society of Australia* 28, 323-332.
14. Denham, D., Windsor, C. R. (1991). The crustal stress pattern in the Australian continent. Tyne, E. & Vozoff, K. (eds.), *Exploration in a changing environment; Australian Society of Exploration Geophysicists 8th conference and exhibition and the Geological Society of Australia exploration symposium; conference papers. Exploration Geophysics*, 22, 101–105.
15. Gallagher, K. (1995). Evolving temperature histories from apatite fission-track data. *Earth and Planetary Science Letters*, 136, 421-435.
16. Gleadow, A., Kohn, B., Belton, D., Raza, A. (2002). Supplementary Report on Geological Observations and Results of Fission Track Thermochronology, Replacement Research Reactor Site, Lucas Heights NSW.
17. Herbert, C. (1980). Depositional development of the Sydney Basin. In: Herbert, C. & Helby, R (editors), A guide to the Sydney basin. *Department of Mineral Resources, Geological Survey of New South Wales, Bulletin* 26, 11-52.
18. Herbert (1988). The Lapstone Monocline-Nepean Fault – A high angle reverse fault system. *TMOC Resources report.*

19. Herbert, C., Helby, R. (editors) (1980). A guide to the Sydney basin. *Department of Mineral Resources, Geological Survey of New South Wales, Bulletin* 26, 603.
20. Humphreys, G. S., Field, R. (1998). Mixing, mounding and other aspects of bioturbation: Implications for pedogenesis. *16th World Congress of Soil Science, CD ROM publication* 18.
21. Huntley, D. J., Godfrey-Smith, D. I., Thewalt, M. L. W. (1985). Optical dating of sediments. *Nature* 313, 105-107.
22. International Atomic Energy Agency (1991), Earthquakes and Associated Topics in Relation to Nuclear Power Plant Siting, Safety Series 50-SG-S1 rev 1.
23. Jacobs, J. A. (1994). Reversals of the Earth's Magnetic Field. *Cambridge University Press, Cambridge.*
24. Lohe, E. M., McLennan, T. P. T., Sullivan, T. D., Soole, K. P., Mallett, C. W. (1992). Sydney Basin – Geological Structure and Mining Conditions, assessment for Mine Planning. *CSIRO Division of Geomechanics, External Report* 20.
25. Mauger, J., Creasey, J.W., Huntington, J.F. (1984). Extracts and notes on the Katoomba 1:100,000 Sheet, Sydney basin fracture analysis. *CSIRO Division of Mineral Physics.*
26. Mayne, S. J., Nicholas, E., Bigg-Wither, A. L., Rasidi, J. S., Raine, M. J. (1974). Geology of the Sydney Basin; a review. *Bulletin Australia Bureau of Mineral Resources, Geology and Geophysics* 149, 229.
27. Mermarian, H., Fergusson C. L. (1994). Fracture pattern of the Illawarra Coal Measures. Southeastern Sydney Basin. Proceedings in the 28th Newcastle Symposium, 151-158.
28. Murray, A. S., Olley, J. M. (2002). Precision and accuracy in the optically stimulated luminescence dating of sedimentary quartz: A status review. *Geochronometrica* 21, 1-16.
29. Murray-Wallace, C.V., Belpario, A.P. (1991). The latest Interglacial shoreline in Australia – A review. *Quaternary Science Reviews,* 10, 441-461.
30. Nicol, A., Berryman, K., Langridge, R., Cox, S., Simpson, K., Volk, P., Hill, N. (2002). ANSTO — Replacement Research Reactor Project Tasks 1 & 2 — Site Fault Assessment. *GNS Client Report* 2002/103.
31. Norman, A. R., Creasey, J. W. (1985). Structural analysis of the Ku-ring-gai-Berowra area. Advances in the study of the Sydney Basin, Proceedings of the nineteenth symposium, *Department of Geology, The University of Newcastle,* 19-24.
32. Ollier, C.D. (1982). The great escarpment of eastern Australia: tectonic and geomorphic significance. *Journal of Geological Society Australia,* 29, 13-23.
33. Opdyke, N. D., Channell, J. E. T. (1996). Magnetic Stratigraphy. *Academic Press, San Diego.*
34. O'Sullivan, P. B., Coyle, D. A., Geladow, A. J. W., Kohn, B. P. (1996). Late Mesozoic to early Cenozoic thermotectonic history of the Sydney Basin and the eastern Lachlan Fold Belt, Australia. *Geological Society of Australia Inc., Extended Abstracts* 43, (Mescozoic Geology of Eastern Australia Plate Conference, Brisbane, September 1996), 424-432.
35. Pillans, B (1998). Regolith Dating Methods - A guide to numerical dating techniques, CRC for Landscape Evolution and Mineral Exploration, ISBN 0 9586857 4 6.
36. Pillans, B., Bourman, R. (1996). The Brunhes/Matuyama polarity transition (0.78 Ma) as a chronostratigraphic marker in Australian regolith studies. *AGSO Journal of Australian Geology and Geophysics*, 16, 289–294.
37. Pillans, B., Bourman, R. (2001). Mid Pleistocene arid shift in southern Australia, dated by magnetostratigraphy. *Australian Journal of Soil Research*, 39, 89–98.
38. Pillans, B. (2002). Paleomagnetic Dating of regolith at Lucas Heights. *Report to the Institute of Geological and Nuclear Sciences*, (September, 2002).

39. Rickwood, P. C. (1985). Igneous intrusives in the Greater Sydney region. In: Pells P.J.N. (editor). *Engineering Geology of the Sydney Region*, 215-307.
40. Sdrolias, M., Muller, R.D., Gaina, C. (2001). Plate tectonic evolution of Eastern Australian Marginal Ocean. *PESA Eastern Australasian Basins Symposium*, 227-237.
41. Shackleton, N. J., Berger, A., Peltier, W. R. (1990). An alternative astronomical calibration of the lower Pleistocene timescale based on ODP Site 677. *Transactions of the Royal Society of Edinburgh*, 81, 251–261.
42. Shepherd, J (2002) pers. comm.
43. Shepherd J., Huntington, J. F. (1981). Geological fracture mapping in coalfields and the stress fields of the Sydney basin. *Journal of the Geological Society of Australia* 28, 299-309.
44. Sherwin, L., Holmes, G. G. (1986). Geology of the Wollongong and Port Hacking 1:100,000 Sheets 9029, 9129 Geological Survey of New South Wales Department of Mineral Resources.
45. Spell, T. L., McDougall, I. (1992). Revisions to the age of the Brunhes/Matuyama boundary and the Pleistocene geomagnetic polarity timescale. *Geophysical Research Letters*, 19, 1182–1184.
46. Stirling, M. W., Berryman, K. R. (2001). Extension to Lucas Heights probabilistic seismic hazard assessment. *GNS Client Report* 2001/85, 27pp.
47. US Nuclear Regulatory Commission, Fault Capability Criteria (in press).
48. Wolfe, R. A., Farley, K. A., Kass, D. M. (1998). A sensitivity analysis of the apatite (U-Th)/He thermochronometer. *Chemical Geology*, 148, 105-114.

Figure 8.3 Apatite fission track data from boreholes at Lucas Heights

Sample number	Number of grains	Standard track density ($\times 10^6$ cm^{-2})	Fossil track density ($\times 10^5 cm^{-2}$)	Induced track density ($\times 10^6 cm^{-2}$)	Uranium content (ppm)	Chi- square probability %	Age dispersion %	Fission track age (Ma) ($\pm 1\sigma$)	Mean track length ± st. error (μm)	Std. dev. (μm)
BH107-A	30	1.120 (3854)	6.152 (554)	1.900 (1711)	21	25.3	4.40	69 ± 4[a]	13.63 ± 0.15 (83)	1.37
BH109-C	20	1.200 (3854)	4.592 (484)	1.451 (1529)	15	99.7	0.00	72 ± 4[b]	14.03 ± 0.13 (39)	0.84
BH 110-B	22	1.280 (3854)	6.324 (531)	2.052 (1723)	20	86.4	0.15	75 ± 4[b]	14.44 ± 0.17 (70)	1.40

Brackets show number of tracks counted or measured. Standard and induced track densities measured on mica external detectors densities on internal mica surfaces.
[a]*Age determined A. Raza calculated using zeta = 384±5 for Corning glass dosimeter CN-5.*
[b]*Ages determined by B.P. Kohn calculated using zeta = 383.5±5 for Corning glass dosimeter CN-5.*
All ages shown are central ages.

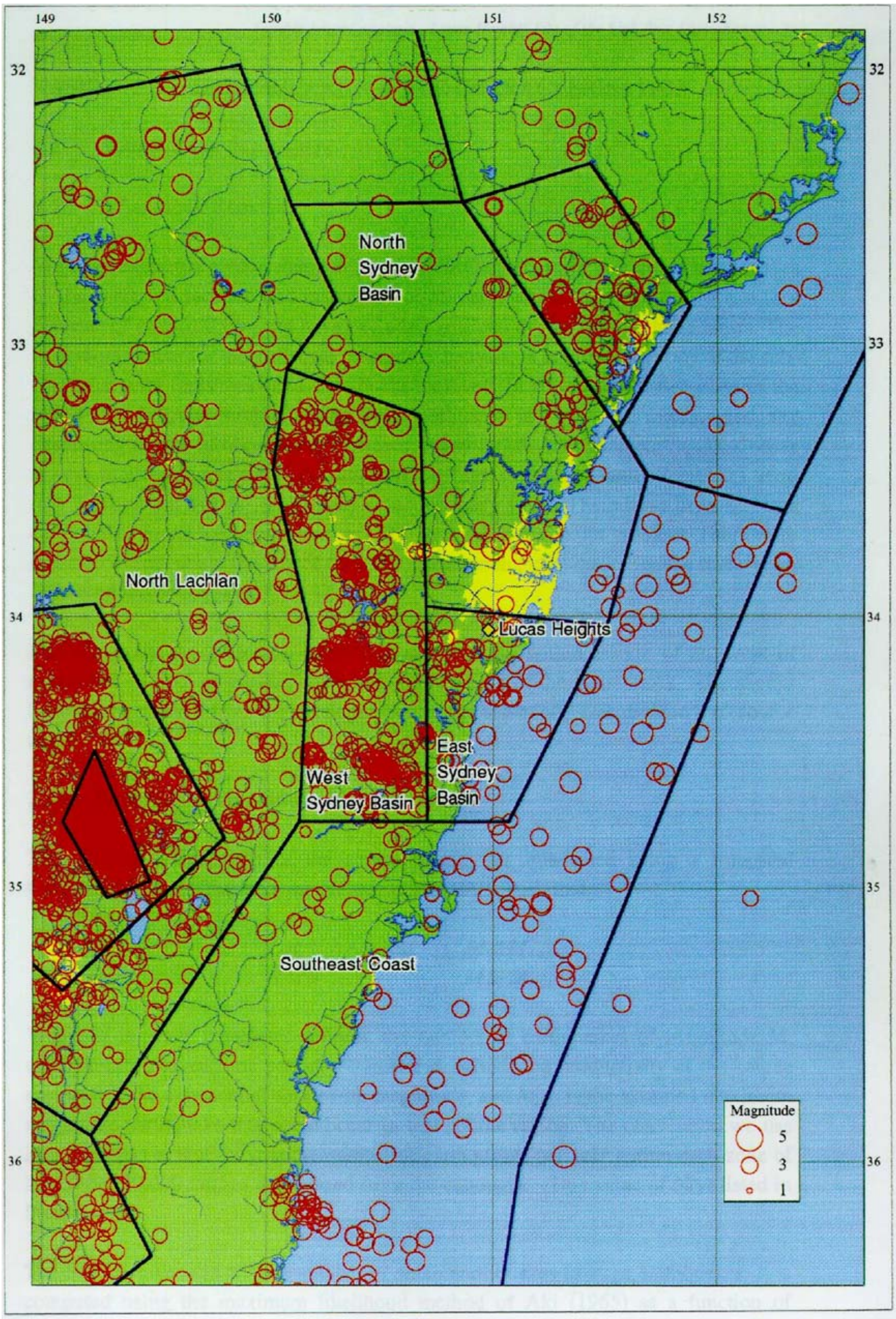

Figure 3.1: Delineation of five earthquake source zones around the Lucas Heights site. (Taken from Alliance, 1999)

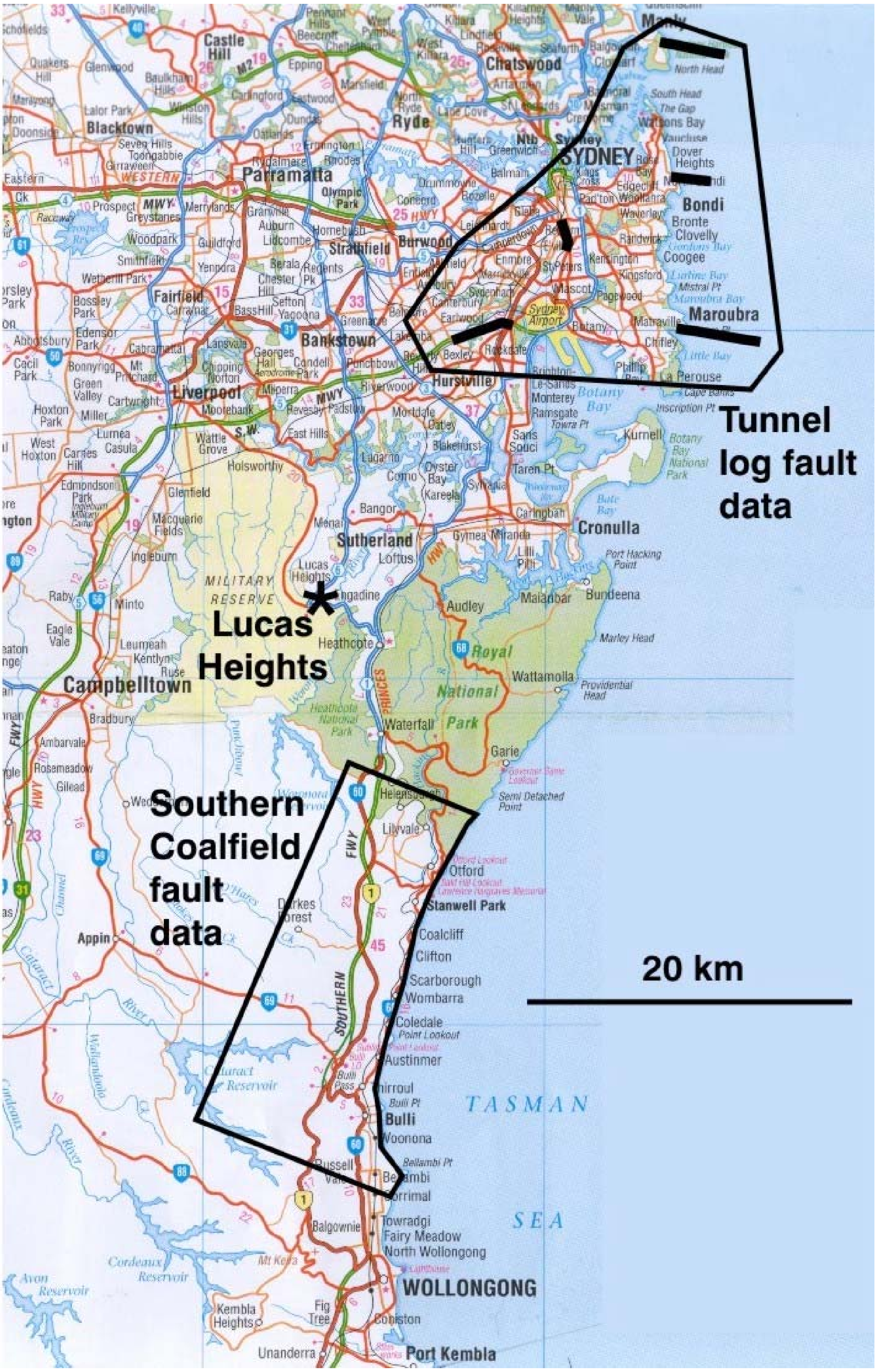

Figure 4.1 – Regional map of Sydney basin (Note: The two M5 tunnels are shown as a continuous line in this figure).

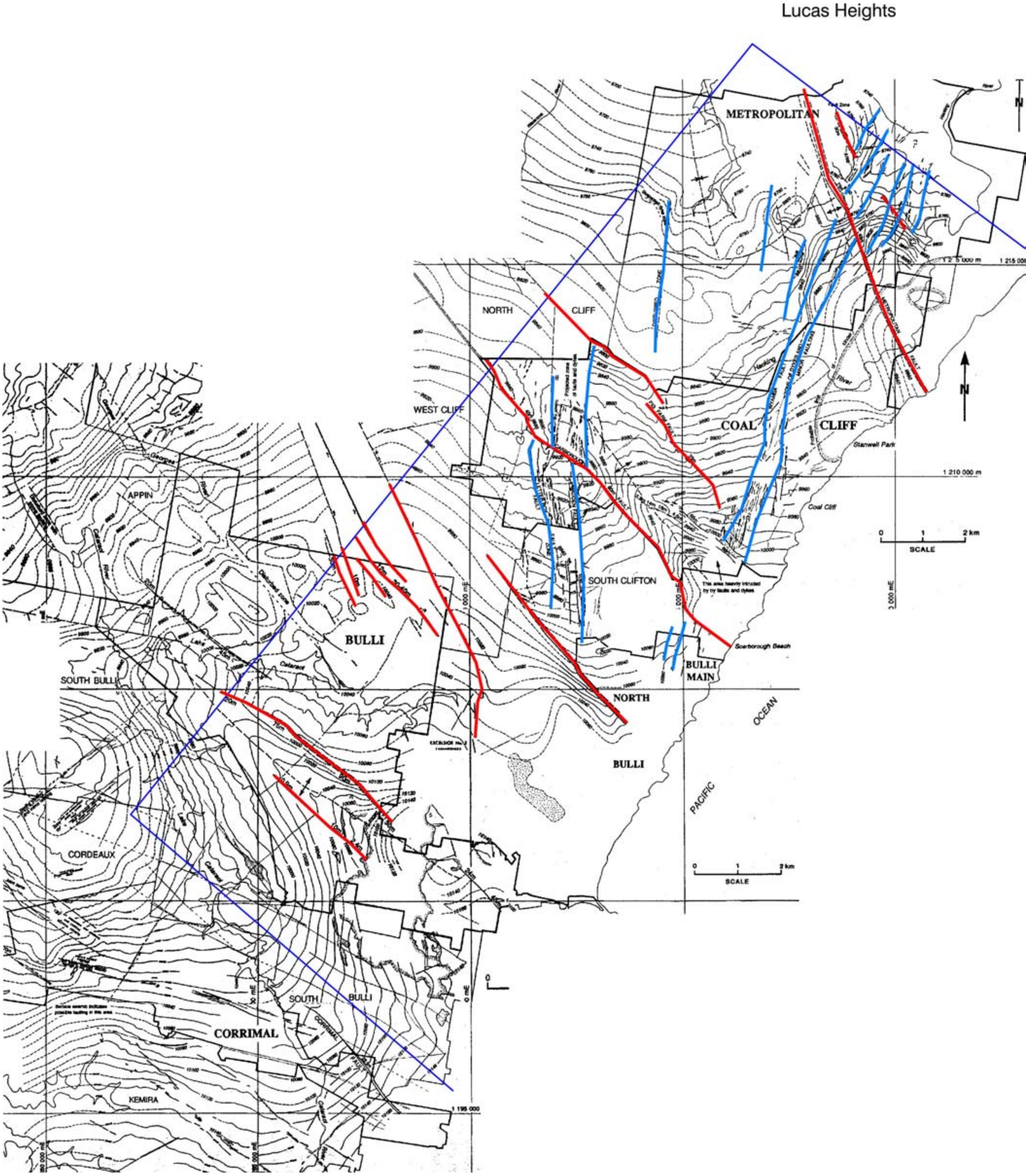

Figure 4.2 – Area from which the southern coalfield fault data was collated.

Figure 4.3 – Location of tunnels in the Sydney region from which faults were recorded. (Note: The two M5 tunnels are shown as a continuous line in this figure).

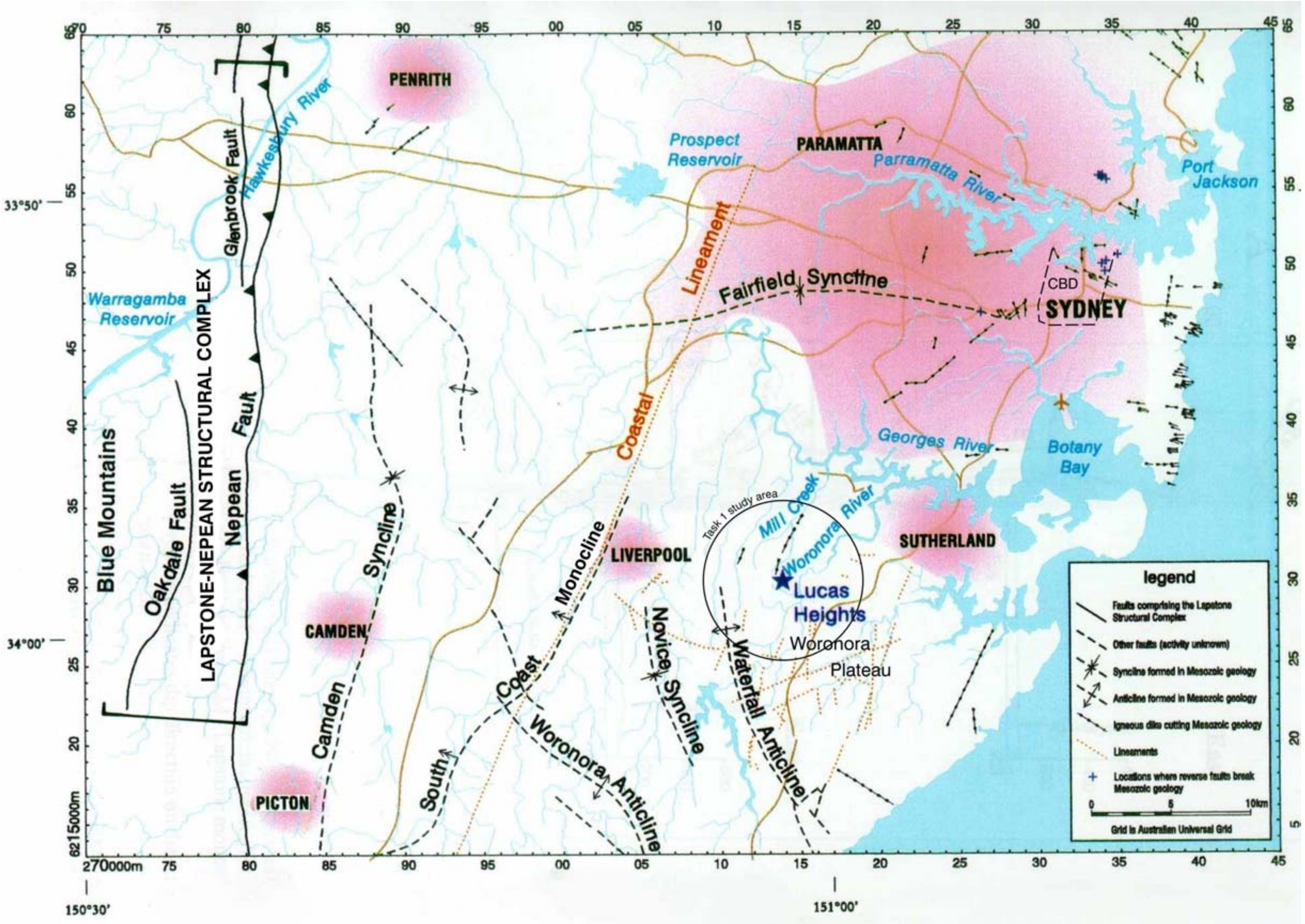

Figure 5.1 – Regional structure geology map showing main fault, folds and lineaments. Location of the Replacement Research Reactor (RRR) site at Lucas Heights is indicated by the star. Pink shows urban areas and CBD refers to Sydney central business district. (Nicol et al., 2002)

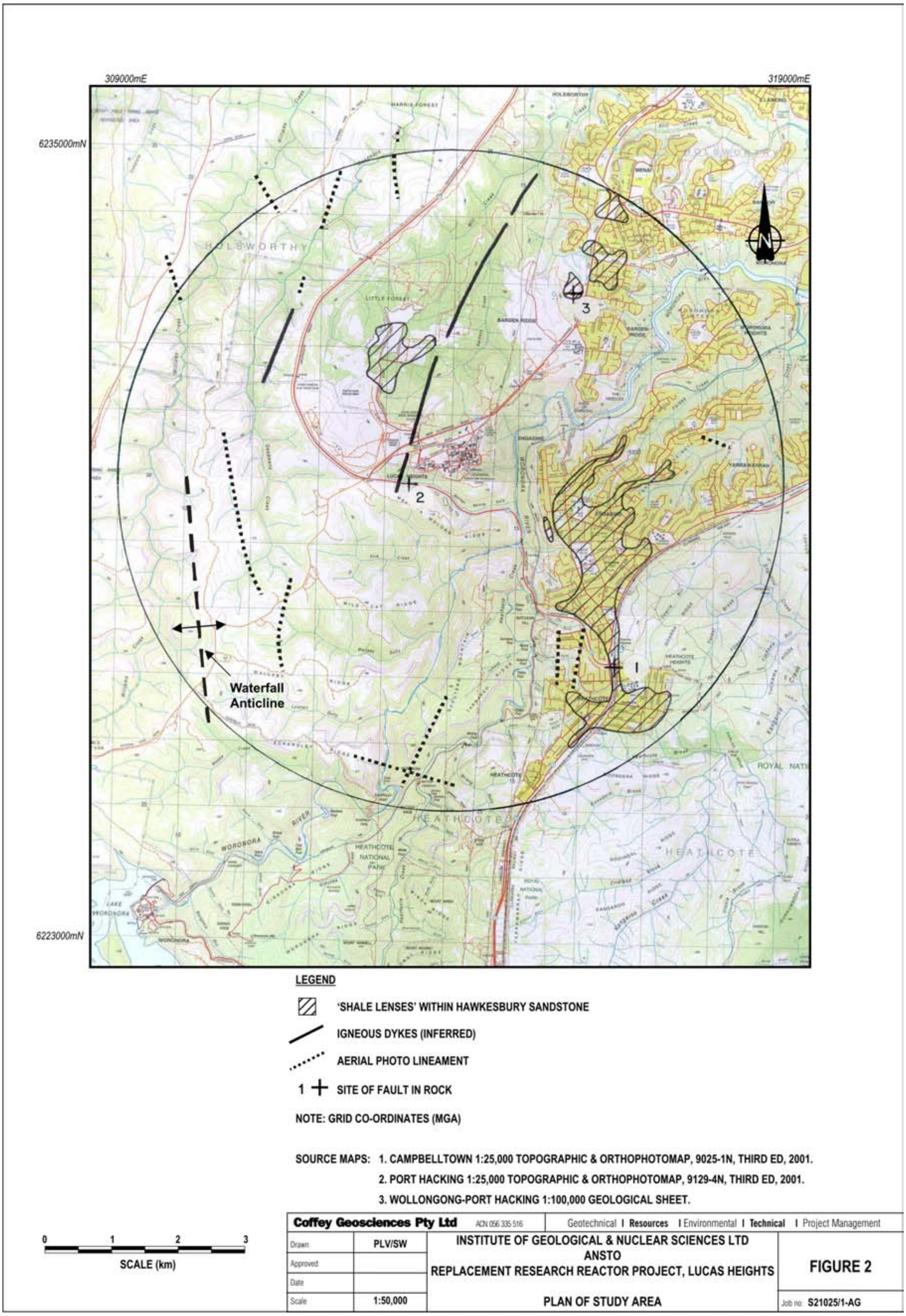

Figure 5.2 – Plan of Near Field Study Area. (Taken from Nicol et al., 2002)

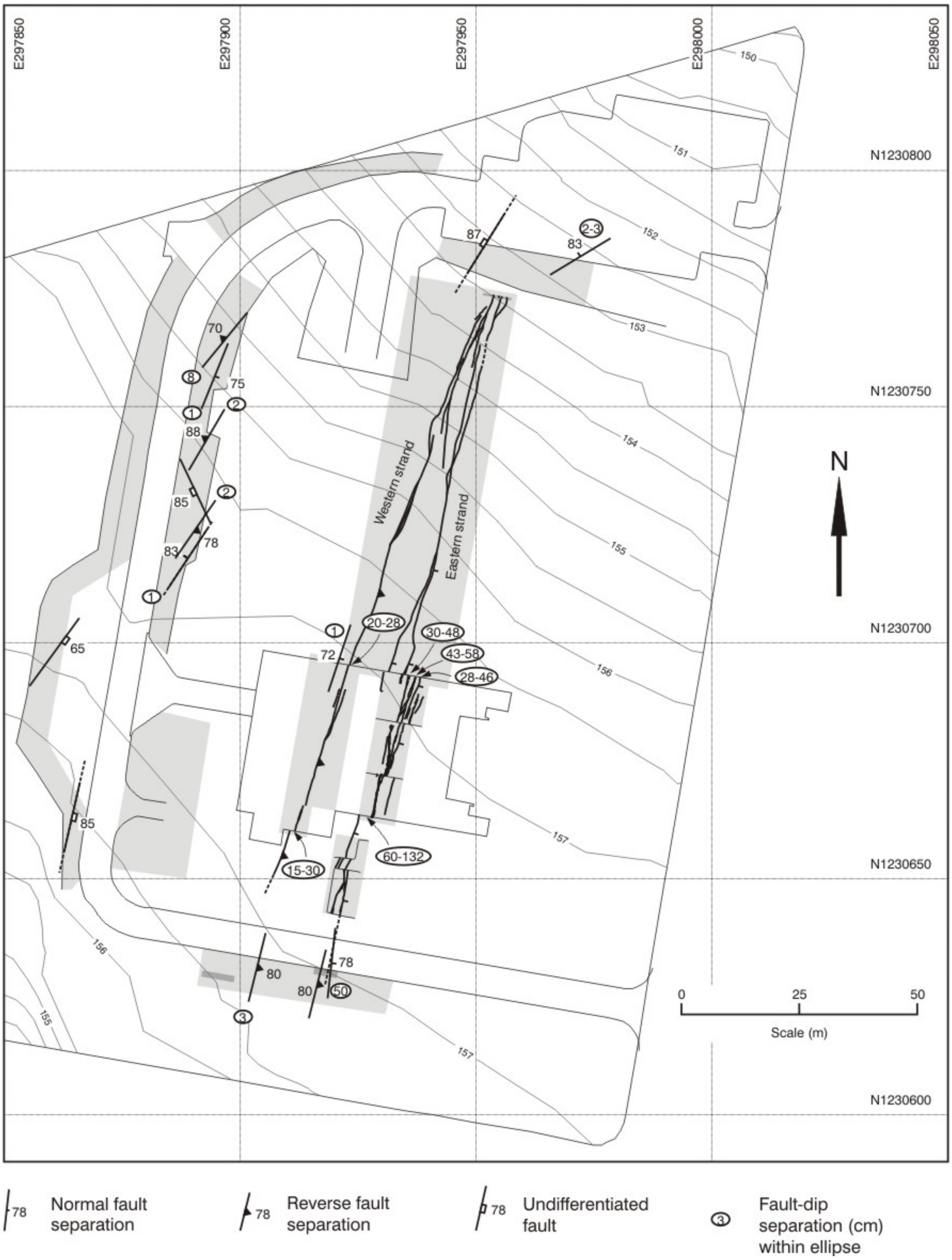

Figure 6.1 – Site map showing the locations of faults. Ticks, teeth, or rectangles on faults show dip direction of fault with dip angles in degrees indicated. (Taken from Nicol et al., 2002)

Figure 6.2 – Photograph of eastern fault strand on southern wall of the reactor building excavation

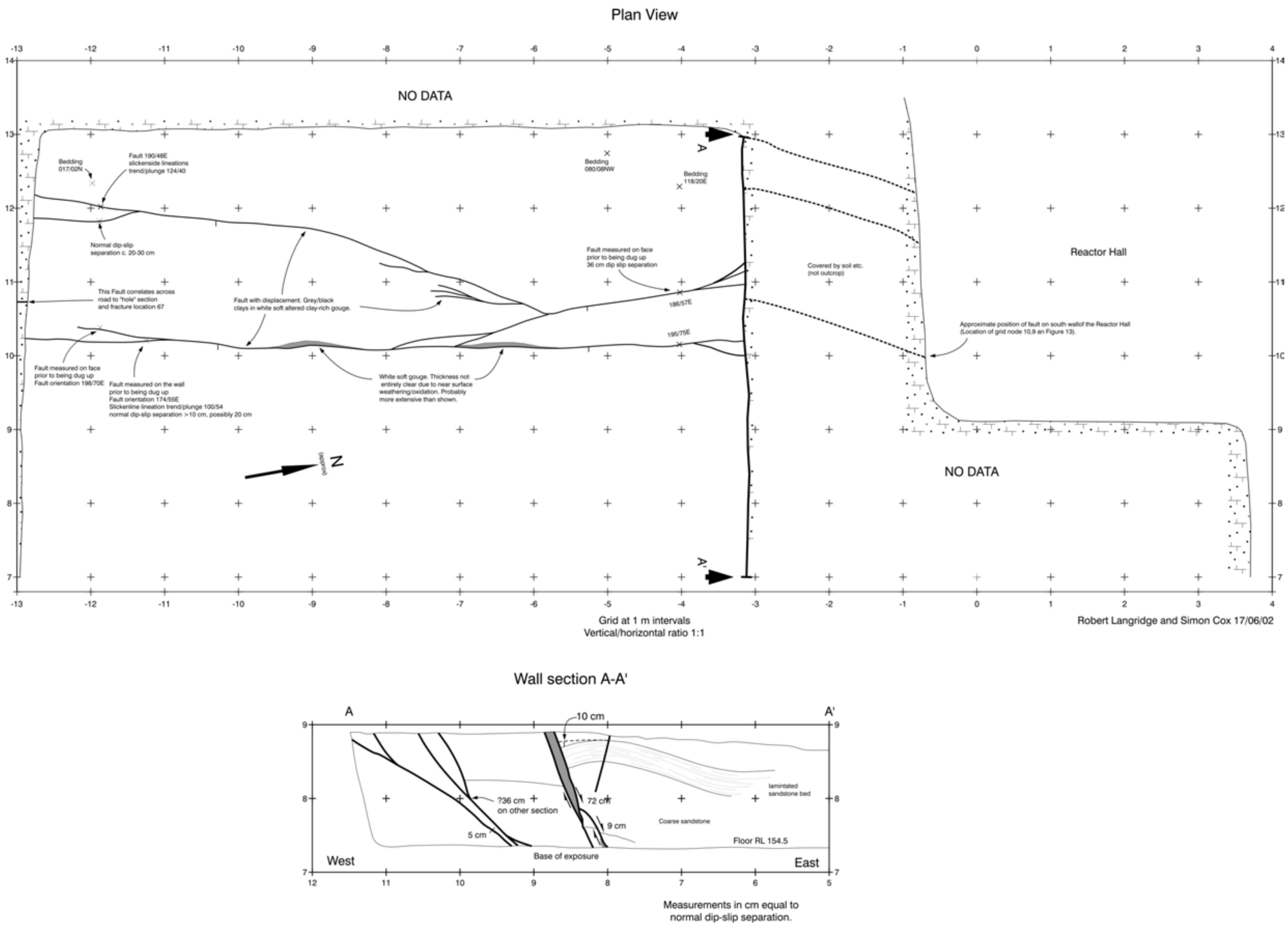

Figure 6.3 – Log of crane excavation site showing both plan (map) view and cross-section. (Taken from Nicol et al., 2002)

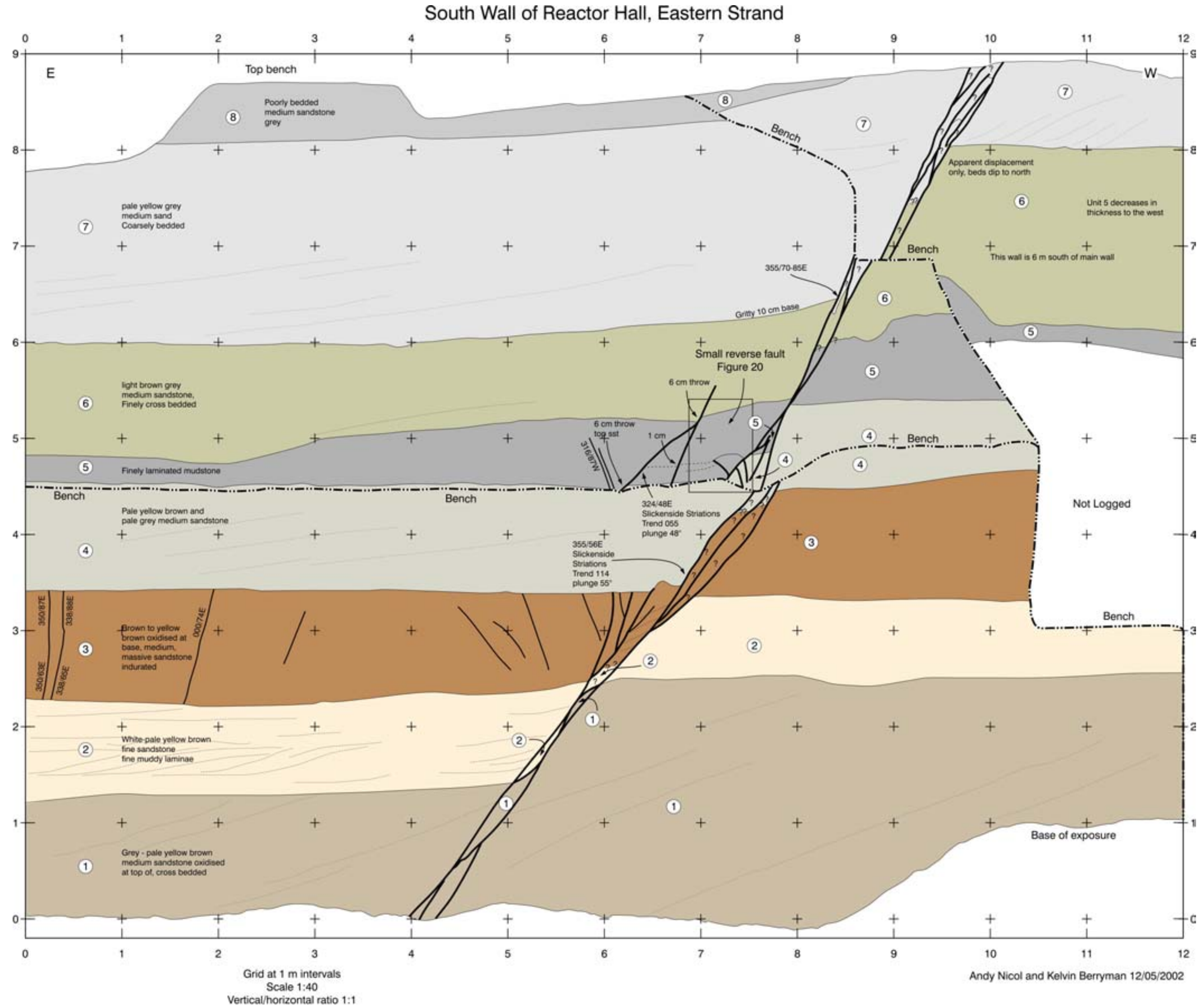

Figure 6.4 – Log of eastern fault strand in the south wall of the reactor building excavation. (Taken from Nicol et al., 2002)

North Wall Reactor Hall, Eastern Strand

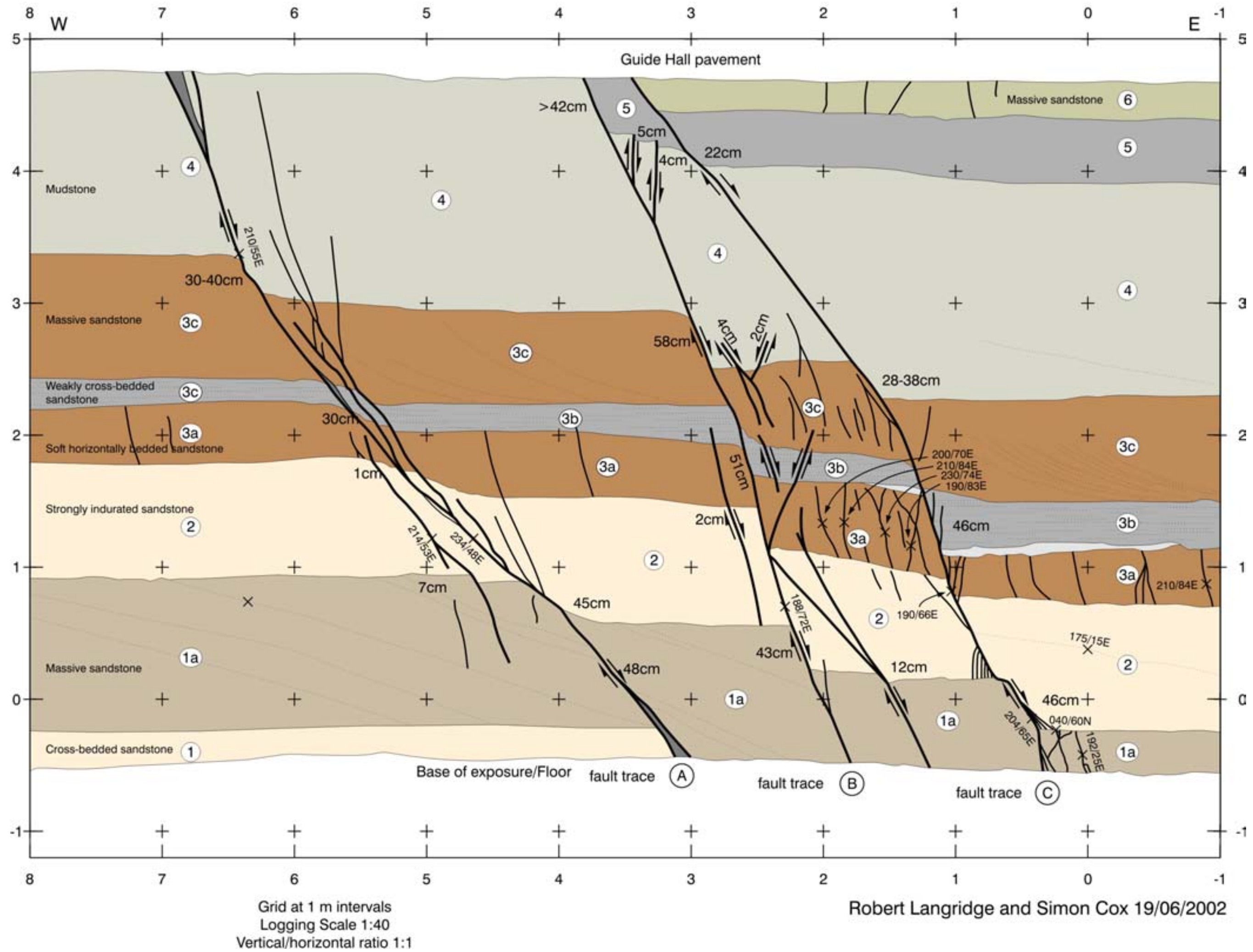

Figure 6.5 – Log of eastern fault strand in north wall of the reactor building excavation. (Taken from Nicol et al., 2002)

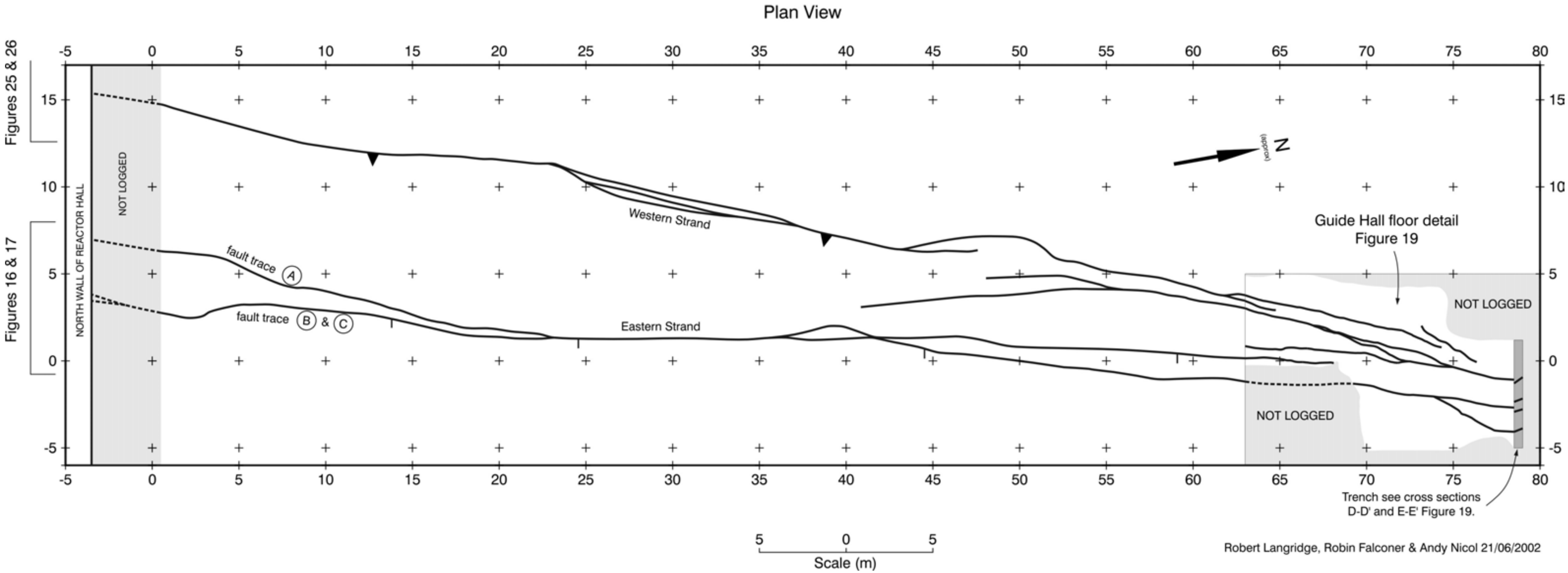

Figure 6.6 – Log of the eastern and western fault strands along the neutron guide hall location. (Taken from Nicol et al., 2002)

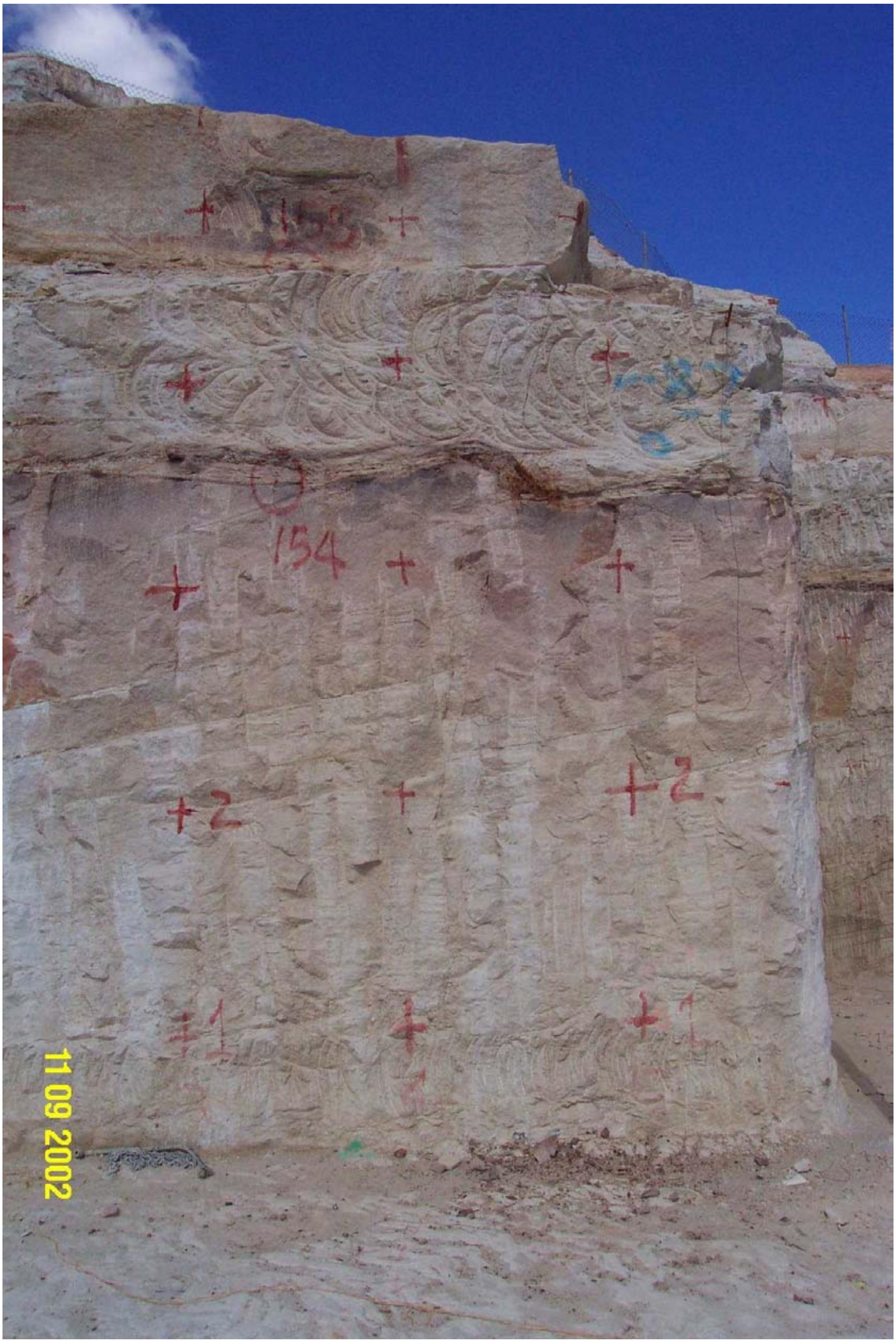

Figure 6.7a – Photograph of western fault strand on southern wall of the reactor building excavation. (Red crosses indicate a 1 metre grid)

Figure 6.7b – Close-up photograph ferruginous layer in western fault strand on southern wall of the reactor building excavation. (Red crosses indicate a 1 metre grid)

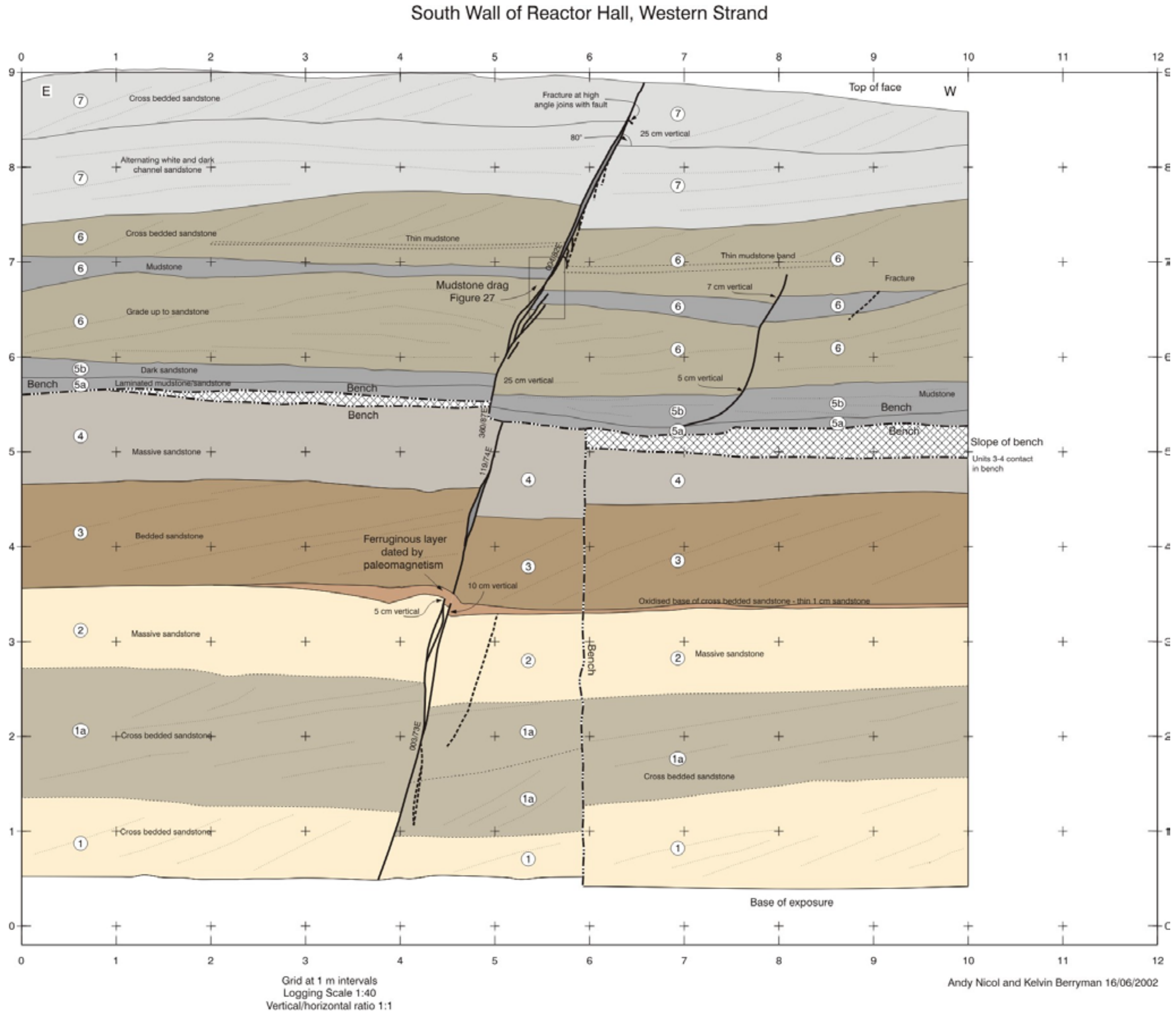

Figure 6.8 – Log of the western fault strand on south wall of the reactor building excavation. (Taken from Nicol et al., 2002)

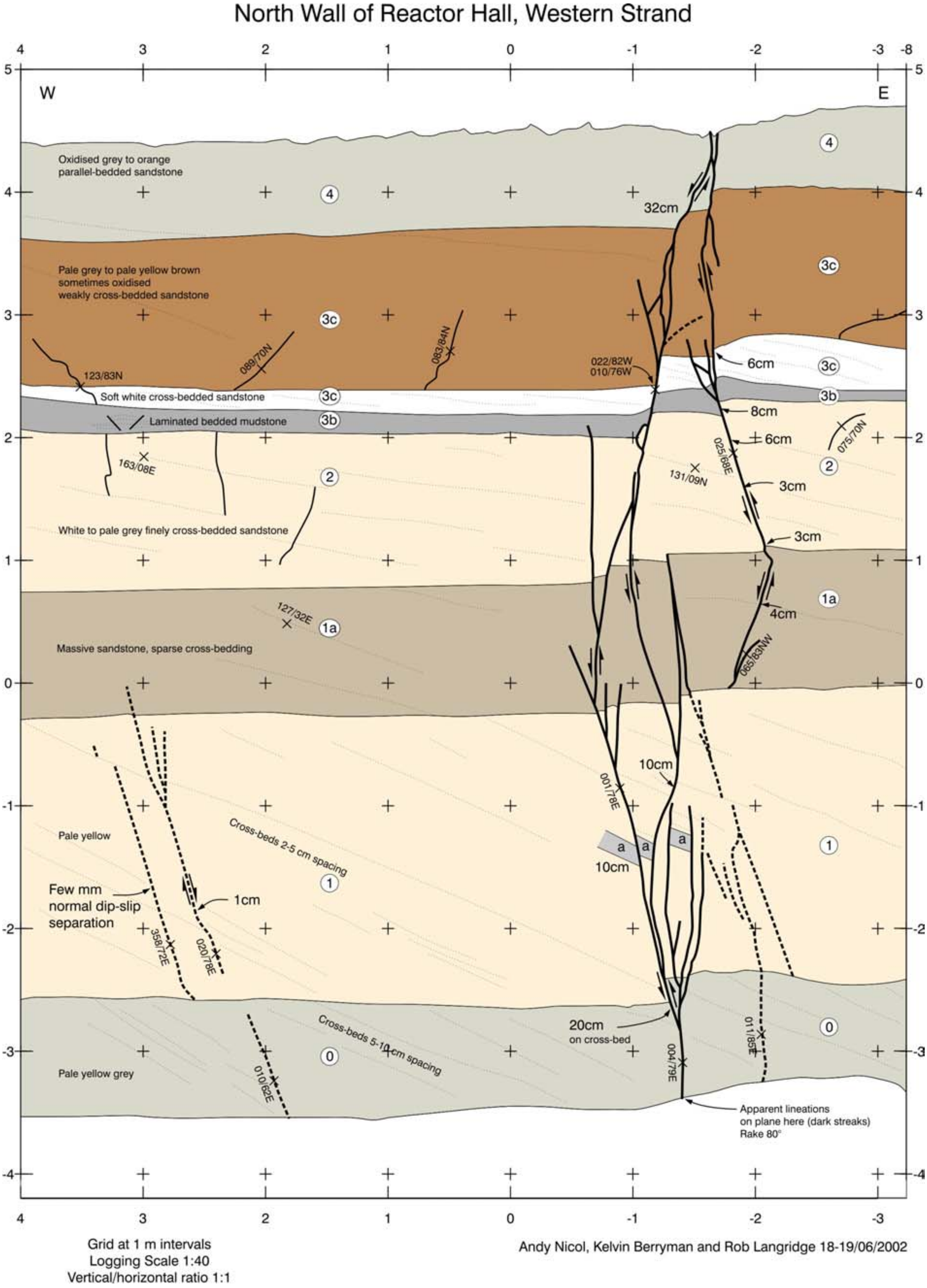

Figure 6.9 – Log of the western fault strand in the north wall of the reactor building excavation. (Taken from Nicol et al., 2002)

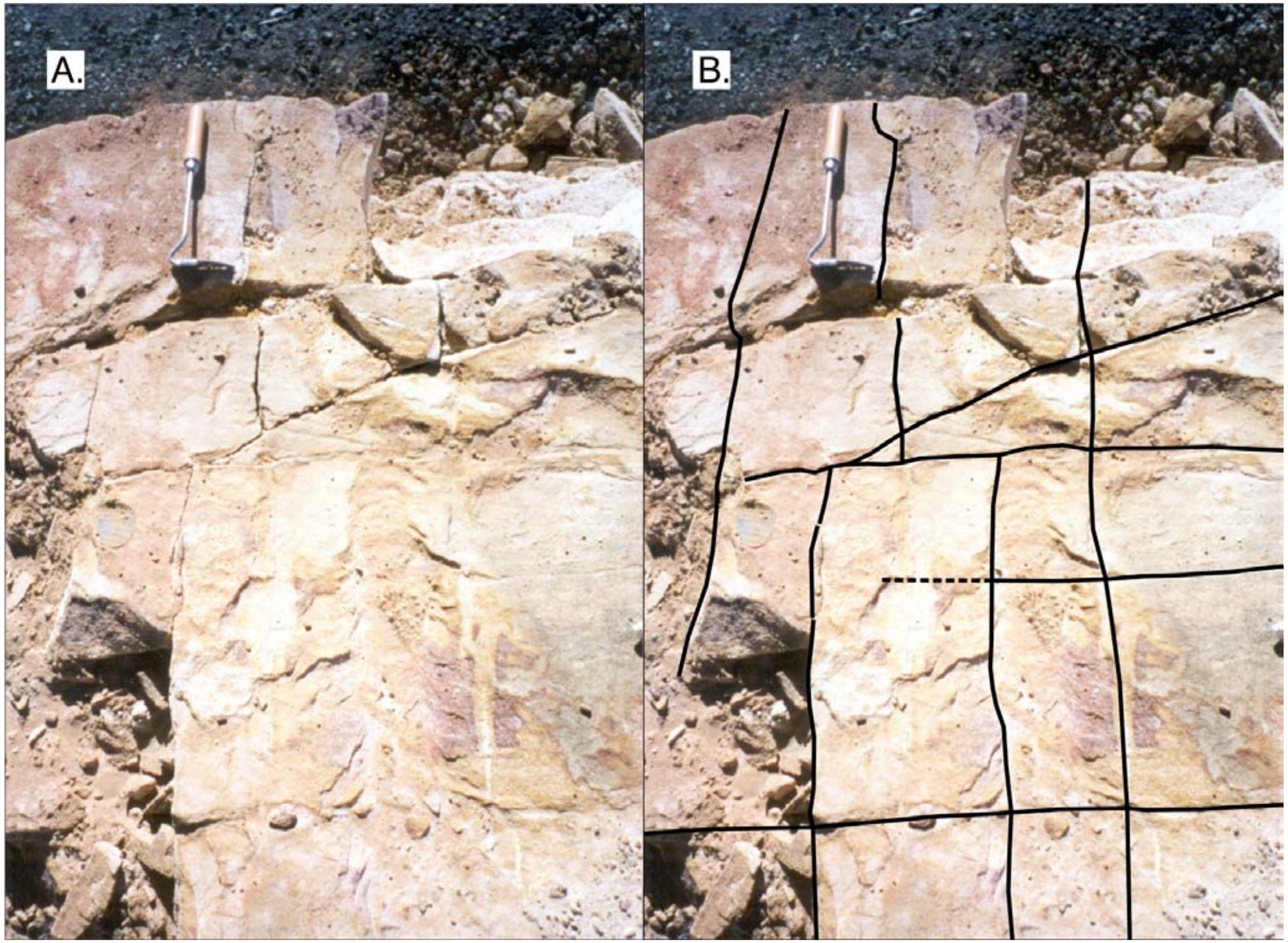

Figure 6.10 – Photograph of orthogonal joints (a) and line drawing over photograph (b) on a small horizontal bedrock pavement. North is to the top of the photograph. Scraping implement is about 30cm long. (Taken from Nicol et al, 2002)

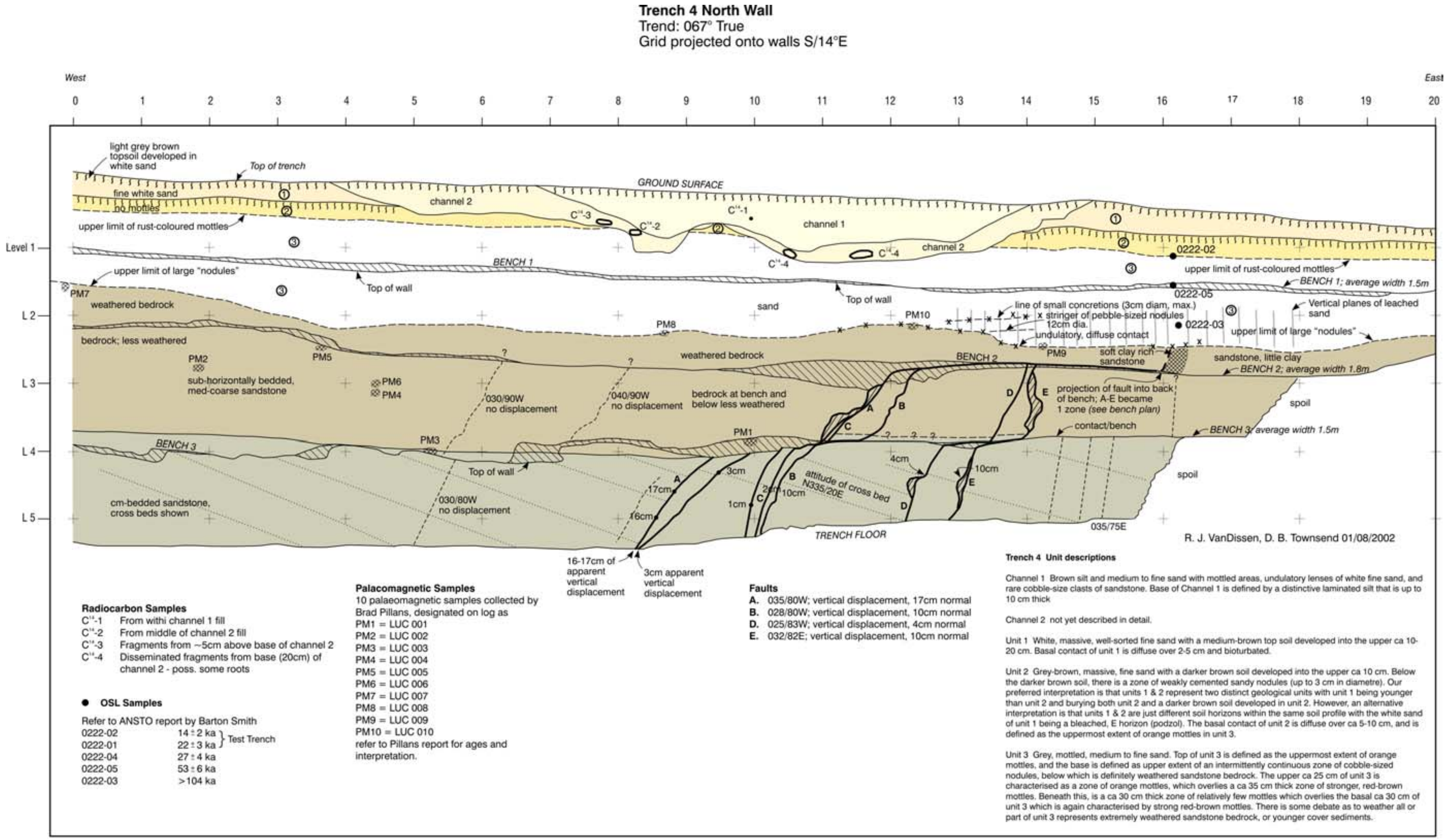

Figure 8.1 - Log of north wall of Trench 4 excavated outside the perimeter fence of the replacement reactor site. The trench is floored by Hawkesbury Sandstone and has a thick cover of Quaternary deposits. The cover deposits and staining have been sampled for paleomagnetic (PM), and OSL (filled circles) dating. (Taken from Langridge et al., 2002)

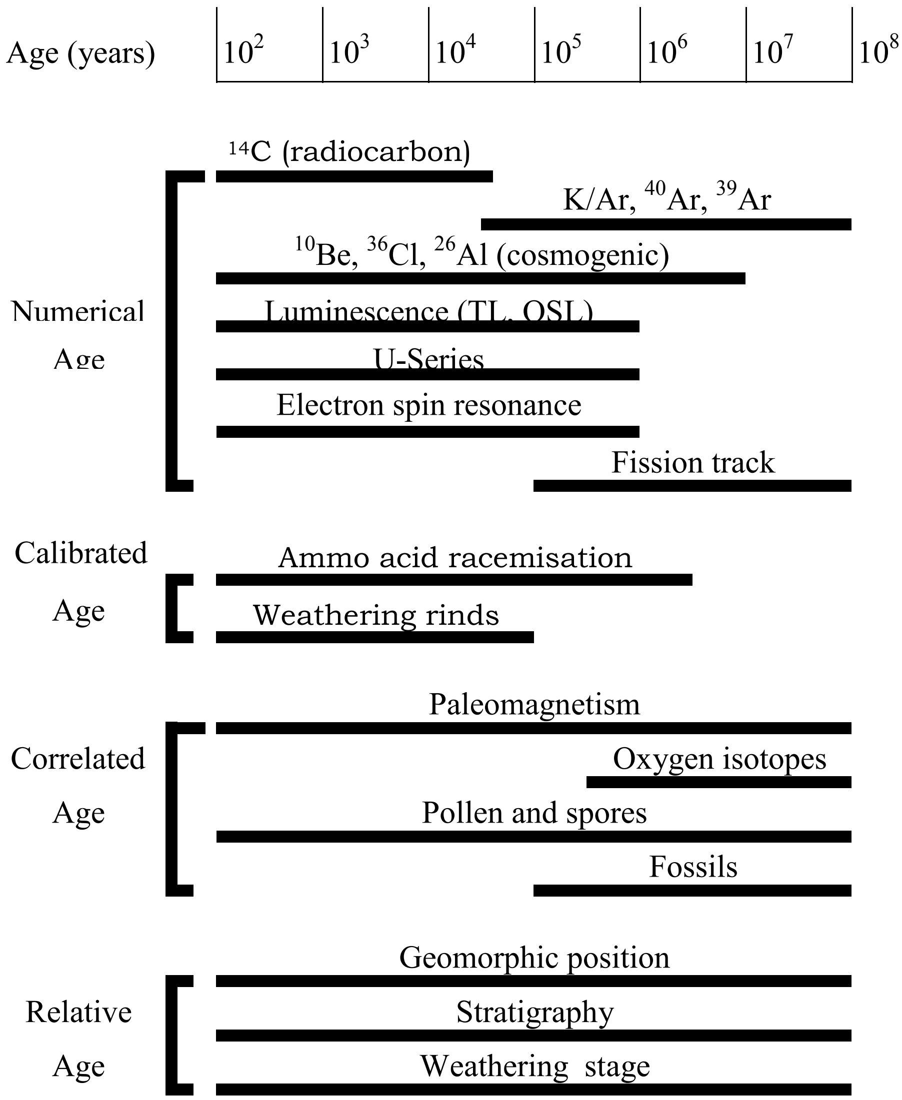

Figure 8.2: Age ranges over which regolith dating methods can be applied. Methods are grouped according to type of age result produced.
(Taken from Pillans, 1998)

GEOMAGNETIC POLARITY TIMESCALE

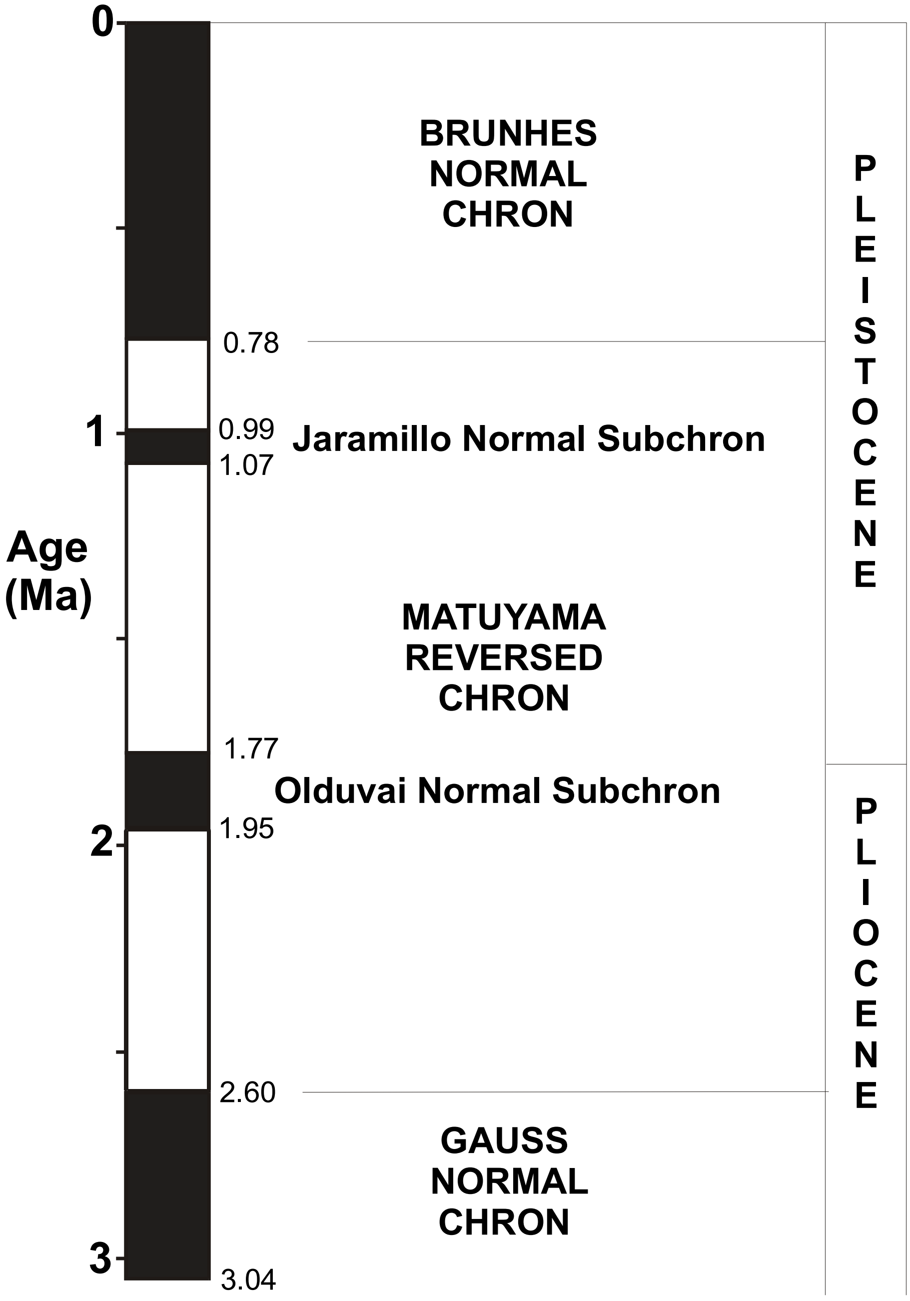

Figure 8.3 – Geomagnetic Polarity Timescale for the last 3 Ma (after Shackleton et al. 1990)

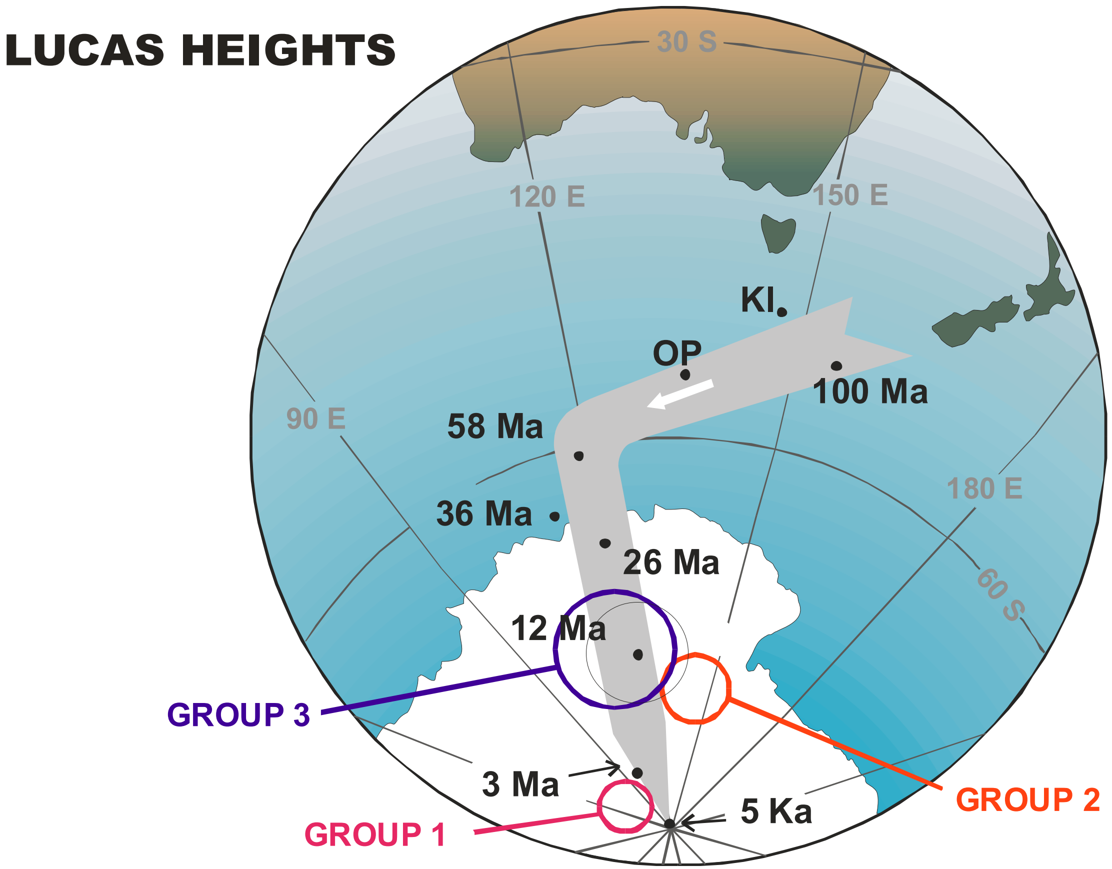

Figure 8.4 – Late Mesozoic to Cainozoic Australian Apparent Polar Wander Path (after Idnurm 1985; 1994), with Lucas Heights paleomagnetic poles (95% confidence circles) shown for Group 1, 2 and 3 specimens (see text). (taken from Pillans, 2002)

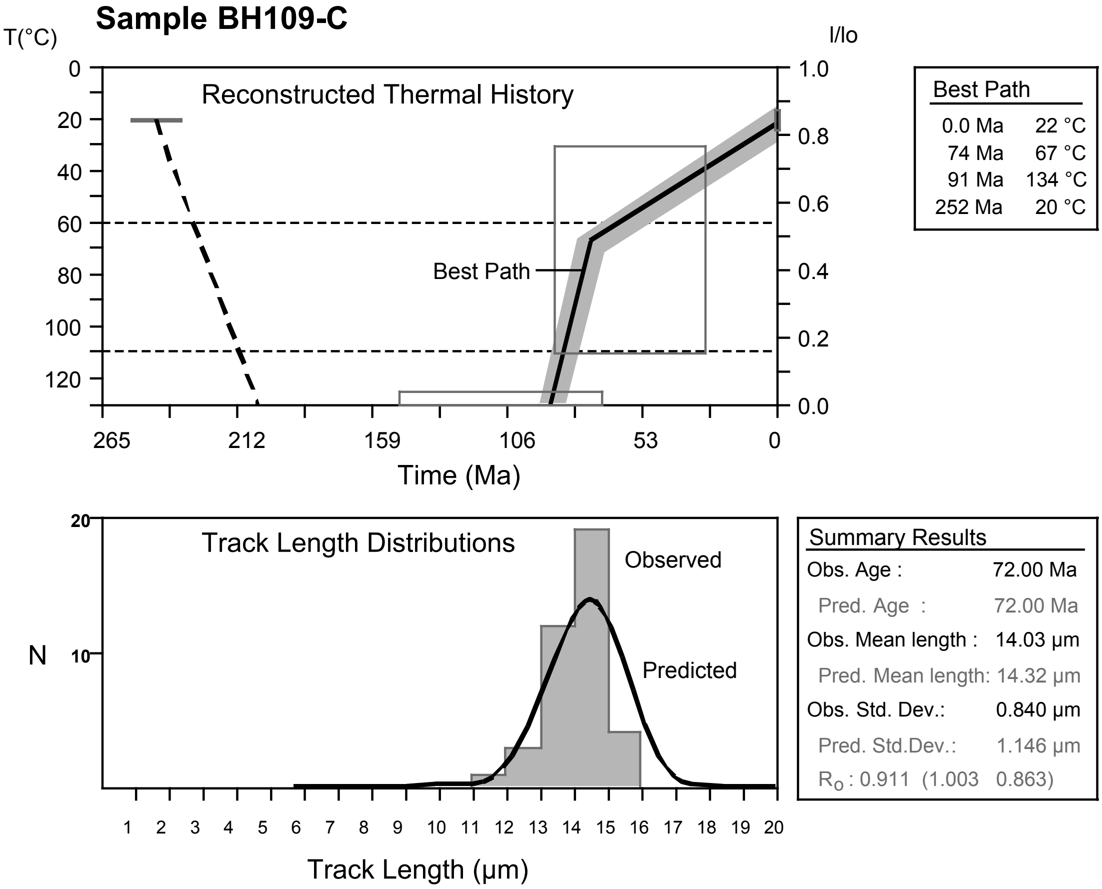

Figure 8.5: Modelled thermal history for apatites from rock sample BH109-C. The upper curve shows the most likely thermal history for this sample which is consistent with the fission track and (U-Th)/He results. The grey band shows the most likely cooling paths and the black line the single best-fit temperature history. Grey boxes on this plot show the initial constraints which were used to limit the possible pathways according to geological evidence. The predictions for the best-fit thermal history are compared with actual measurements in the lower boxes.